IDENTIFYING AND MODELING THE DYNAMICS OF A CORE CANCER SUB-NETWORK

BAYLEYEGN YIBELTAL N.

IDENTIFYING AND MODELING THE DYNAMICS OF A CORE CANCER SUB-NETWORK

BAYLEYEGN YIBELTAL N.

This dissertation is submitted to the School of Mathematical Sciences, Faculty of Science and Agriculture, University of KwaZulu-Natal, Durban, in fulfillment of the requirements for the degree of Master in Science.

December 2011

As the candidate's supervisor, I have approved this dissertation for submission.

Signed: Professor K S GOVINDER December 2011

Abstract

Many recent studies have shown that the initiation of human cancer is due to the malfunction of some genes at the R-checkpoint during the G_1-to-S transition of the cell cycle. Identifying and modeling the dynamics of these genes has a paramount advantage in controlling and, possibly, treating human cancer. In this study, a new mathematical model for the dynamics of a cancer sub-network concentration is developed. Positive equilibrium points are determined and rigorously analyzed. We have found a condition for the existence of the positive equilibrium points from the activation, inhibition and degradation parameter values of the dynamical system. Numerical simulations have also been carried out. These results confirm analyses in the literature.

Declaration

I declare that the contents of this dissertation are original except where due reference has been made. It has not been submitted before for any degree to any other institution.

BAYLEYEGN Yibeltal Negussie

December 2011

Declaration 1 - Plagiarism

I, BAYLEYEGN Yibeltal Negussie, declare that

1. The research reported in this thesis, except where otherwise indicated, is my original research.
2. This thesis has not been submitted for any degree or examination at any other university.
3. This thesis does not contain other persons data, pictures, graphs or other information, unless specifically acknowledged as being sourced from other persons.
4. This thesis does not contain other persons' writing, unless specifically acknowledged as being sourced from other researchers. Where other written sources have been quoted, then:
    a. Their words have been re-written but the general information attributed to them has been referenced
    b. Where their exact words have been used, then their writing has been placed in italics and inside quotation marks, and referenced.
5. This thesis does not contain text, graphics or tables copied and pasted from the Internet, unless specifically acknowledged, and the source being detailed in the thesis and in the References sections.

Signed 

Acknowledgments

First of all I would like to express my deepest appreciation to my advisor, Professor K S Govinder, without whose guidance and persistent help this thesis would have not been possible. I thank him for his welcoming attitude, exceedingly valuable comments and ideas, and unlimited patience that developed in me confidence and courage to achieve my aim of doing problem solving research. I also owe a huge thank to him for the tremendous opportunity offering me to present research results at many conferences including at Mathematical Biosciences Institute, (MBI), Ohio, USA. Moreover, I thank him for his careful and painstaking proof reading of the manuscripts. Professor Govinder epitomizes all the qualities that one seeks from ones advisor, but that are rarely found in a single person.

My particular thanks to AIMS and the School of Mathematical Sciences, UKZN for funding this research work covering fee structure, accommodation and living costs. I also would like to thank all the academic and management staff of the School of Mathematical Sciences at UKZN for welcoming me, for all kinds of assistance and diverse facilities.

My special thanks goes to my wife, Hirut Assaye, and our daughter, Afomia Yibeltal for their patience, encouragement and understanding. Without the help and the understanding of my wife at every step of the way, this research work would have not been a successful one. I am also very grateful to Dr. Molla and his wife Mrs. Nafkot for their support and personal advice along the way.

Dedication

To the Almighty God

To my wife Hirut

To my daughter Afomia.

Contents

Chapter 1

Introduction

In this chapter, first we define systems biology and present some of the key biological concepts necessary to motivate and develop our mathematical model. We then introduce the human body cell and its cell cycle. We continue further to briefly discuss how the tumor cell progresses. We also discuss the types of genes, their corresponding network and functions at the R-checkpoint in the literature review section. We then finally discuss about the new cancer subnetwork and the objective of the study.

1.1 Background to Systems Biology

Systems biology is an approach by which biological questions are addressed through integrating experiments, mathematical modeling and simulations [33]. The objective of systems biology is the understanding of the dynamical interactions between components of a living system, between living systems and their interactions with the environment. Systems biology deals with the network of interacting proteins including (i) the reception and emission of chemical signals within and between cells, (ii) the modulation and integration of signals which control gene expression and ultimately cell function, and (iii) the control and coordination of metabolic processes responsible for the intracellular bioenergetics and the biosynthesis. Modeling is not the final goal of systems biology, but is a tool to enhance the understanding of the system, to

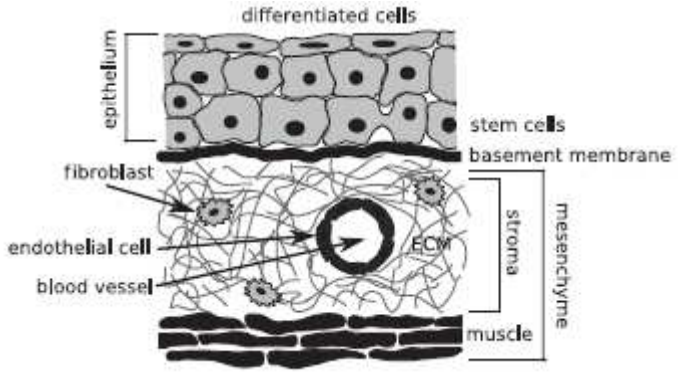

Figure 1.1: Typical tissue microarchitecture showing epithelium separated from the stroma by a basement membrane [10].

develop more directed experiments and finally to allow predictions [33]. Cell functions such as cell differentiation, apoptosis, and the cell cycle are a prototypical focus of systems biology.

1.2 Human Body Cells and the Cell Cycle

The mammalian tissue structure is mainly composed of epithelial cells, the stroma, and the mesenchymal cells [10]. The epithelium is composed of sheets of tightly adhered epithelial cells which are separated by the basement membrane from the stroma. The stroma is a loose connective tissue, which is interlaced by blood vessels, nerves, and lymphatic vessels. The stroma includes the extracellular matrix (ECM) and the fibroblast of the cell which have a vital role in the progression of the cancer cell. The mesenchymal cell is a combination of the stroma and the muscle as shown in Figure 1.1. This complex structure of a cell is maintained and regulated by a signal network that integrates genetic and proteomic information with extracellular signals received through membrane-bound receptors [10].

1.2.1 Cell Population Dynamics

Each cell type population is regulated by balancing proliferation and apoptosis (we discuss proliferation and apoptosis of a cell in the next section). When a differentiated cell dies, then a

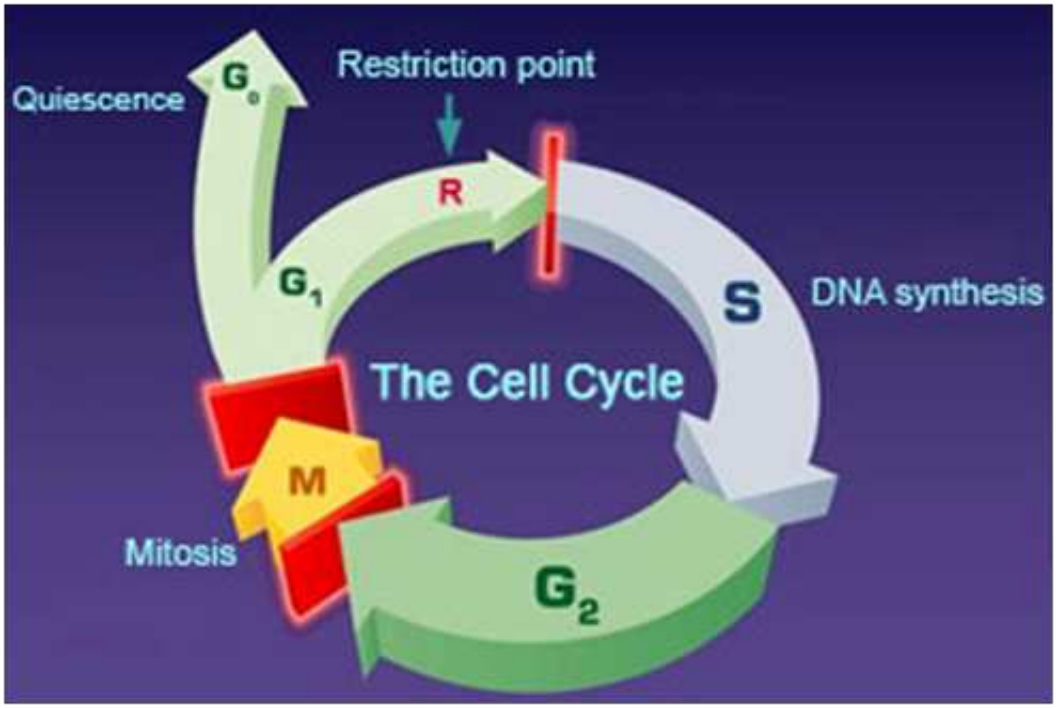

Figure 1.2: Phases in mammalian cell cycle [6].

somatic cell divides either symmetrically or asymmetrically. The division will give two new stem cells in the first case while a stem cell and a progenitor cell in the latter case. The progenitor cell either further divides or terminates its differentiation and is pushed to the correct position to assume its normal function. All these processes are controlled and organized by intercellular communication through biochemical signals and mechanics [10].

1.2.2 Cell Cycle, Proliferation and Apoptosis

The Eukaryotic cell cycle is a repeated sequence of events that enable the division of a cell into two daughter cells. The cell cycle is classically divided into four phases: gap 1 (G_1), synthesis (S), gap 2 (G_2), and mitosis (M). The diagramatic representation of the cell cycle is given in Figure 1.2. There are specific activities which are carried out in each phase of the cell cycle while the cell undergoes cell division. In the G_1 phase of the cell cycle, the cell physically grows, proteins are synthesized, new organelles are constructed, and the cell prepares for DNA replication. In the following S phase the DNA is copied while in the G_2 phase final preparations

for cell division are made within the nucleus of the cell. In the last phase, M, the cell divides into two daughter cells, which then begin a new cycle of division [5, 10, 18, 42].

The cell cycle contains numerous checkpoints that allow the cell to check for and repair DNA damage, as well as to control or halt cell progression. At the R-checkpoint either the cell commits to division and then progresses to the S phase or exits the cell cycle and enters the quiescent state (G_0). There are also checkpoints in between the G_2 and the M phases to detect and repair DNA damage. Cells that fail to repair DNA damage at such checkpoints induce apoptosis (a cellular program which results in cell death) [10]. The cell cycle process is orchestrated by production and balance of chemical signals (principally Cyclins and Cyclin-dependent kinases (Cdk_s)) that activate and inhibit the cell cycle progression genes, which form a complex and highly integrated network [10]. Basically, the cyclins (Cyclin E, cyclin D) activate the signals while Cdk_s inhibits the cell cycle progression in the early stage of G_1 by forming the inactive form of Cyclin/Cdk complex. In this network, activating and inhibitory signal molecules interact, forming positive feedback loop (when the signal transduction of one step in the network facilitates the effect of the other signal transduction steps in the network) and negative feedback loops (when the signal transduction of one step in the network hinders effect on the other signal transduction steps in the network), which ultimately control the dynamics of the cell cycle. The correct interpretation of growth and inhibitory signals is key to maintaining the normal cell cycle process. The two types of genes which are particularly important in regulating cell proliferation are oncogenes (which respond to or create growth signals and promote cell cycle progression such as Cyclins and Cdk_s) and tumor suppressor genes (TSG_s) (which respond to inhibitory signals, retard or halt the cell cycle, or to ensure DNA repair such as Cdk inhibitor families ($P27^{Kip1}$, INK4)). If either of these genes or both malfunction, then cancer initiation (carcinogenesis) will occur.

1.3 The Biology of Cancer

Cancer occurs when defective genes cause cells to malfunction and interact with the body in an aberrant manner by either increasing cell proliferation or decreasing cell apoptosis [2, 3, 10, 18]. The initiation of cancer may require the accumulation of multiple mutations which allow cells to break out of the regulatory networks which ensure cooperation. Once a cancerous cell has been created, it can undergo a process known as clonal expansion (gives rise to descendants by cell division). This enables it to ignore growth-inhibiting signals from its neighbors, bypass its internal controls and checkpoints, and form a colony of hyperproliferative aberrant cells.

1.3.1 Avascular, Vascular Growth and Metastasis

Once a tumor has established a foothold in its host tissue, in its early stage, it depends upon the host vasculature for crucial substrates [10]. Substrates (such as oxygen, nutrient, and growth factors) diffuse from the surrounding vascularized host tissue to the tumor and are uptaken by proliferating tumor cells. The tumor cell interacts with the microenvironment of the body cell both mechanically and chemically. It interacts with the body cell mechanically by displacing and compressing the surrounding tissue including the basement membrane. It also interacts chemically by secreting enzymes such as matrix metallo proteinases (MMP_s) that degrade ECM.

Many studies have reported that acidosis (a decreased microenvironmental pH level resulting from anaerobic glycosis in hypoxic tumor cells) plays a role in tumor invasion by inducing apoptosis in the surrounding epithelium and contributing to the ECM degradation [10, 21]. The ultimate result of cancer development is angiogenesis, where the tumor induces endothelial cells to form a new vasculature that directly supplies the tumor cell. This supply of substrate allows tumor cells to enter the blood supply, travel to a different site, and start growing in different organs of the body. This process is referred to as metastasis [10].

1.4 Literature Review

In mammals, entry into DNA replication is guarded by a cell cycle checkpoint called Restriction (R)-checkpoint; a name proposed by Pardee [31]. Pardee conducted experiments to demonstrate the R-checkpoint as a unique switching point between quiescent and proliferative states of normal animal cells. A series of time-lapse video analyses has also been carried out by Zetterberg and Larsson [41] to determine the precise location of the R-checkpoint. It occurs in the mid-to-late G_1 phase and marks the transition from mitogen-dependant to mitogen-independent progression of the cell cycle [3]. The suggestion of Pardee [30, 31] that the R-checkpoint has a vital importance in preventing malignant transformation has gained substantial support from detailed genetic and molecular studies reported in recent years [3]. As a result, it has been reported that the cell cycle is suspended at the R-checkpoint if the cell has not grown sufficiently or possesses damaged DNA [2]. Once the cell does not qualify to progress to the S phase, it resides in the quiescent state (G_0 state) and is induced to re–enter the cell cycle by mitogenic stimulation.

Many human cancers are known to originate from the malfunction of some genes at the R-checkpoint such as transcriptional factors (E2F, C-Myc), cyclins (D, E), cyclin-dependent kinases (Cdk_s), retinoblastoma protein (Rb), phosphatase Cdc25A and cyclin-dependent kinases inhibitor $P27^{Kip1}$ [2, 3, 18, 42]. D-type cyclins (D1, D2, D3) serve as targets of growth factors to integrate extracellular signals into the core cell cycle regulators [18]. These cyclins are induced to express in response to a variety of mitogenic signals and function as a regulatory subunit of cyclin-dependent kinases (Cdk2, Cdk4, Cdk5, Cdk6). On the other hand, cyclin E (CycE) and transcription factor E2F, are directly involved in the initiation of chromosomal DNA replication [5, 18]. It has been claimed that almost all cancers are associated with one or more mutations of genes at the R-checkpoint [29]. Examples include the following: (i) inactivation of Rb in breast and cervical cancers and CML carcinoma, (ii) loss of cyclin-dependent kinase inhibitor $P16^{INK4a}$ in pancreatic cancer, (iii) overexpression of CycD, CycE or Cdk4 in breast, head and neck cancers, and (iv) loss of $P27^{Kip1}$ in breast, prostate, colon, lung, and esophagus cancers [39].

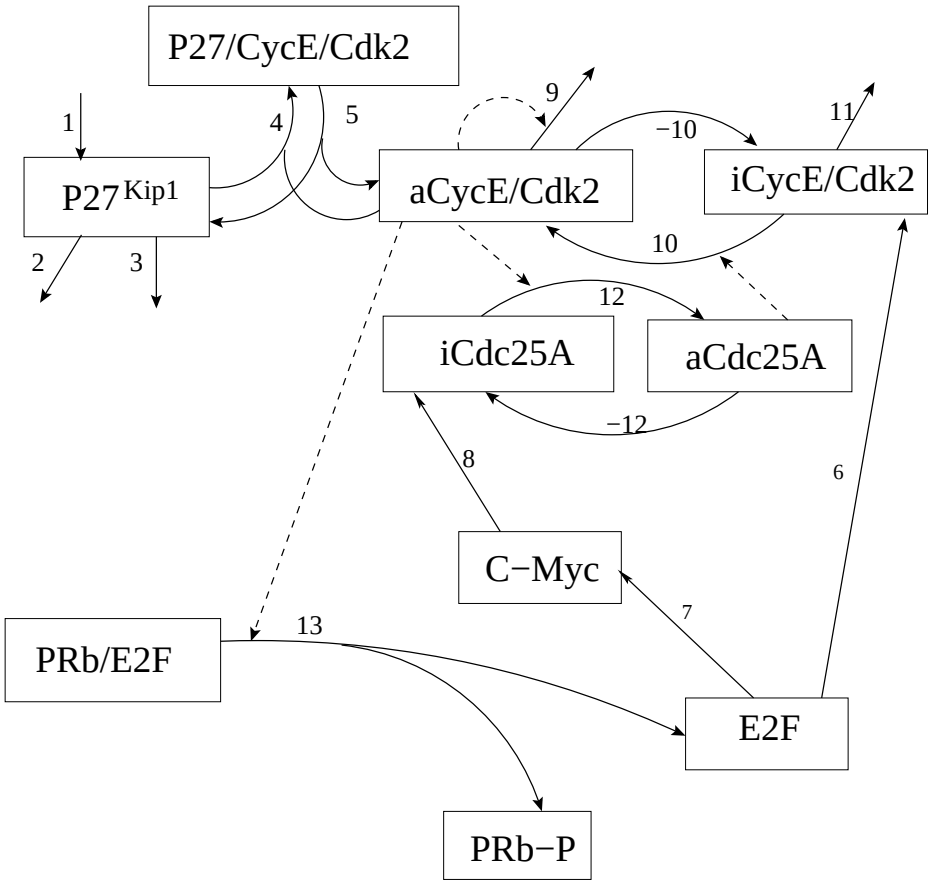

Figure 1.3: Schematic model of part of the molecular signaling involved in the regulation of the G_1-to-S transition [3].

Given the complexity of the cell cycle, a logical approach is to model the G_1-to-S and the G_2-to-M transitions separately. The biological reason for this approach is the existence of two strong checkpoints: the R-checkpoint between the G_1 and S phases and the G_2/M-checkpoint between the G_2 and M phases. Mathematical models of regulation of the G_1-to-S transition have been developed and simulated [3, 15, 42], where the most detailed was developed by Aguda and Tang [3].

Figure 1.3 summarizes the key interaction between the molecular signaling involved among CycE/Cdk2, phosphatase Cdc25A, and Cdk inhibitor $P27^{Kip1}$ during the G_1-to-S transition, which have been identified experimentally over the last two decades. All the solid arrows (curves) which are numbered, represent the processes of transcriptional stimulations or activa-

tions while the dashed arrows (curves) which are not numbered, represent the catalytic effect of the regulators on the target processes. To give the general overview of the network and the individual reaction in the network, we discuss each process as follows:

Process 1 represents the expression of $P27^{Kip1}$ by mitogenic signals [16] which downregulation is given by process 2 which is independent of the Cdk2 kinase activity and process 3 which is dependent of the Cdk2 kinase activity [35]. Processes 4 and 5 represent the binding nature of $P27^{Kip1}$ with CycE/Cdk2 complex to form trimeric complex and its phosphorylation respectively. In our model, to simplify the complexity, we assume that $P27^{Kip1}$ binds only with active CycE/Cdk2 (aCycE/Cdk2) and aCycE/Cdk2 is activated by only the active Cdc25A (aCdc25A). The transcription factor E2F members (E2F1, E2F2, E2F3) have several important target genes that drive cells into the S phase. Some of these are Cyclin E, C-Myc and phosphatase Cdc25A [28]. Process 6 represents the E2F family dependent induction of inactive CycE/Cdk2 complex while processes 7 and 8 represent the transcriptional induction of E2F on C-Myc and the mitogenic stimulation of C-Myc on Cdc25A respectively [11]. Processes 9 and 11 represent the degradation of CycE/Cdk2 complex. Furthermore, it is also shown that aCycE/Cdk2 complex induces its own degradation (curved dashed arrow in process 9) [32]. Process -10 represents the binding nature of CycE and Cdk2, which form an inactive complex with Cdk2 phosphorylate at threonine 14 (Thr^{14}) and tyrosine 15 (Tyr^{15}). The activation of CycE/Cdk2 complex by the catalytic effect (dephosphorylating of Thr^{14} and Tyr^{15}) of Cdc25A is represented by process 10. Process 12 and -12 represent the activation and inactivation activity of phosphatase Cdc25A respectively. In the early G_1 phase, PRb is in a hypophosphorylated (active) form and is able to bind the members of the E2F family of transcription factors. The dashed arrow from aCycE/Cdk2 impinging on process 13 represents PRb phosphorylation. In this process, PRb becomes hyperphosphorylated which leads to its activation and then the release of E2F.

An important feature of the network in Figure 1.3 is the presence of positive feedback loops such as the loop consisting of E2F, process 6, process 10 and the PRb-phosphorylation by aCycE/Cdk2 complex. The other positive feedback loop in the network is composed of the CycE/Cdk2 complex, phosphatase Cdc25A along with the dashed arrows impinging on process

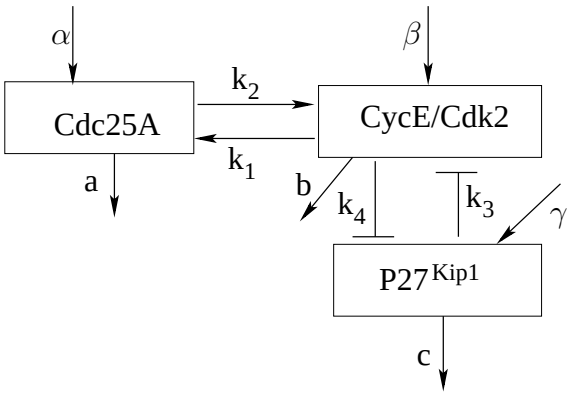

Figure 1.4: A cancer sub-network: All solid arrows represent either gene expression, or activation, or catalytic effect, or degradation effect by itself. The hammerheads refer to inhibition of translation.

12 and process 10, which are reactions that catalyze process 12 and process 10 respectively [17, 35]. These feedback loops account for the sudden increase in CycE/Cdk2 activity which is assumed to stimulate entry into the S phase.

1.5 Cancer Sub-Network Considered in Our Model

Over the last two decades, mathematical models that provide insights into the dynamical mechanisms underlying the cell cycle have been developed [1, 3, 13, 14, 15, 26, 27, 38, 42]. Cell cycle dynamics have been modeled as limit cycles [14, 15, 26, 42], bistable and excitable systems [38, 42], and transient processes [1, 3, 42].

In our study, we have taken the approach of breaking down the regulatory network of the G_1-to-S transition into individual signaling modules, with components active cyclin E-Cdk2 (CycE/Cdk2) complex, active phosphatase protein Cdc25A, and Cdk inhibitor $P27^{Kip1}$. To simplify the network given in Figure 1.3, we merge the active and the inactive form as one module. As a result we obtain the cancer subnetwork in Figure 1.4. The key components of the network that generate a dynamic switching behavior associated with the R-checkpoint include a positive feedback loop between CycE/Cdk2 complex and Cdc25A phosphates, along

with a mutual negative interaction between the cyclin dependent kinases inhibitor P27^{Kip1} and CycE/Cdk2 complex has been identified.

To the best of our knowledge, although the dynamics of the cell cycle during the G_1-to-S transition has been modeled and simulated, the search for a particular type of gene that needs to be manipulated to treat cancer has yet to be concluded. Identifying the key regulatory components during this process and finding out the parameters that need to be manipulated has a vital importance in treating human cancer. In this study, we identify the crucial components (phosphatase Cdc25A, CycE/Cdk2 complex, and P27^{Kip1}) during the G_1-to-S transition of the cell cycle and the key parameters that need to be manipulated to retard the overexpression of Cdc25A or CycE/Cdk2 complex or to reverse the downregulation of P27^{Kip1} level.

1.6 Objectives of the Study

The objectives of this study are (i) to identify some key regulatory components at the R-checkpoint during the G_1-to-S transition of the cell cycle, (ii) modeling the dynamics of their concentrations, and (iii) to identify the parameter(s) need to be manipulated to hinder the overexpression or to reverse the downregulation of the components during the cell cycle process.

Chapter 2

An Overview of Dynamical Systems

In this chapter we discuss some model reaction mechanisms, which mirror a large number of real reactions, and some general types of reaction phenomena with their corresponding mathematical analyses. Understanding these reaction mechanisms is essential in constructing and analysing our cancer sub-network model. We introduce the concept of nondimensionalisation and phase plane analysis to obtain the qualitative behavior of the solution of both linear and nonlinear systems. We further discuss the nonlinear (2-dimensional) systems of differential equations along with the conditions for stability of their equilibrium points. We also discuss the Routh-Hurwitz criteria to determine the stability nature of the equilibrium points for a nonlinear system in higher dimensional space. Finally, we introduce the Bendixson condition to check the existence of a limit cycle solution for a given system.

2.1 Basic Enzyme Reaction

Cells live in a complex environment and can sense different signals, including physical parameters (such as temperature, osmotic pressure), biological signaling from extracellular medium, beneficial nutrients, and harmful chemicals. Cells respond to the information about damage to DNA, membrane, or protein by producing appropriate proteins that act upon the internal or external environment. This information-processing function, which determines the rate of

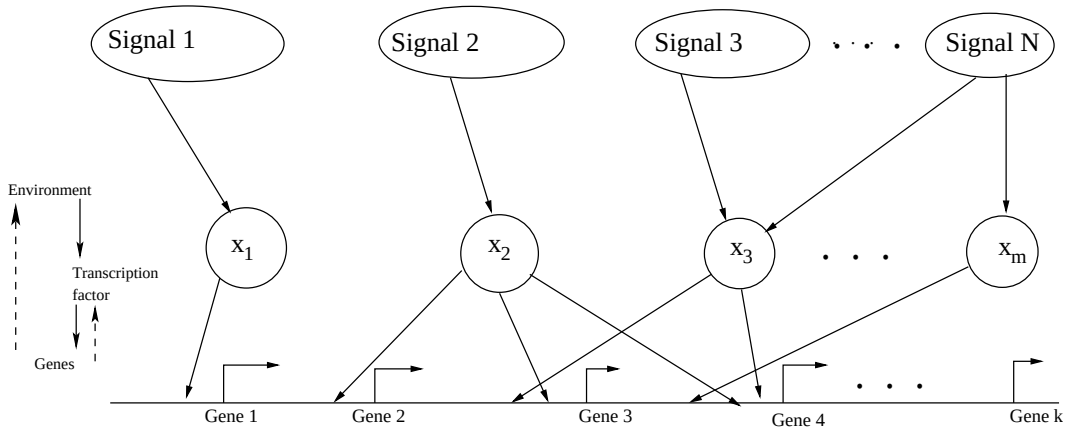

Figure 2.1: The mapping between environment signals, transcription factors inside the cell, and the genes that they regulate. The environmental signals activate the specific transcription factor proteins. An activated transcription factor bind to specific target genes to change the transcription rate at which mRNA is produced. The mRNA is then translated into protein [33].

production of each protein is mainly carried out by transcription networks. Transcription factors are designed to transit rapidly between active and inactive molecular states, at a rate that is modulated by a specific environment signal (input). Each active transcription factor can bind the DNA to regulate the rate at which specific genes are transcribed. The genes which are transcribed into mRNA is then translated into protein to act on the internal and external environment of a cell.

Biochemical reactions are continually taking place in all living organisms and most of them involve proteins called enzymes. Enzymes react selectively on definite compounds called substrates. The enzymes are particularly important in regulating biochemical processes such as activation or inhibition of chemical reactions. To understand their role we have to study the kinetics, which is mainly the study of rates of reactions, the temporal behavior of various reactants and the conditions which govern them [25].

One of the most basic enzymatic reactions, first proposed by Michaelis and Menten [24], involves a substrate (S) reacting with an enzyme (E) to form a complex (SE) which in turn is converted

into a product (P) and an enzyme. The representation of this reaction is

$$S + E \underset{k_{-1}}{\overset{k_1}{\rightleftarrows}} SE \xrightarrow{k_2} P + E \tag{2.1}$$

where k_1, k_{-1} and k_2 are nonnegative constant parameters associated with the rates of reaction. The double arrow symbol $\leftrightarrows$ indicates that the reaction is reversible while the single arrow $\rightarrow$ indicates that the reaction is only one way. Reaction (2.1) states that when one molecule of S combines with one molecule of E, it forms one molecule of SE which eventually produces one molecule of P and one molecule of E again. We denote the concentration of the reactants in reaction (2.1) as follows:

$$[S] = s, \quad [E] = e, \quad [SE] = c, \quad [P] = p, \tag{2.2}$$

where [ ] represents concentration of the substrate.

Definition 2.1.1. The Law of Mass Action states that the rate of a reaction is proportional to the product of the concentrations of reactants [25]. ■

The law of mass action applied to reaction (2.1) leads to the system of nonlinear differential equations

$$\frac{ds}{dt} = -k_1 es + k_{-1} c, \tag{2.3}$$

$$\frac{de}{dt} = -k_1 es + (k_{-1} + k_2) c, \tag{2.4}$$

$$\frac{dc}{dt} = k_1 es - (k_{-1} + k_2) c, \tag{2.5}$$

$$\frac{dp}{dt} = k_2 c. \tag{2.6}$$

To make the mathematical formulation complete, we impose initial conditions on the system of differential equations (2.3)–(2.6) which are given by

$$s(0) = s_0, \quad e(0) = e_0, \quad c(0) = 0, \quad p(0) = 0. \tag{2.7}$$

Now, (2.6) can be decoupled from the system and can be solved as

$$\int_0^t \frac{dp}{dt'} dt' = \int_0^t k_2 c(t') dt' \tag{2.8}$$

which gives

$$p(t) = k_2 \int_0^t c(t')dt', \tag{2.9}$$

once $c(t)$ has been determined.

Moreover, in reaction (2.1), the enzyme E is a catalyst, which only facilitates the reaction, so the total concentration of the enzyme (free and combined with substrate), is constant. This conservation of enzyme is obtained by adding (2.4) and (2.5). Thus

$$\frac{de}{dt} + \frac{dc}{dt} = 0 \quad \text{for all} \quad t \geq 0, \tag{2.10}$$

which implies

$$e(t) + c(t) \equiv K \quad \text{for all} \quad t \geq 0, \tag{2.11}$$

where K is a constant real number. In particular,

$$e(0) + c(0) = K = e_0. \tag{2.12}$$

Therefore,

$$e(t) + c(t) = e_0 \quad \text{for all} \quad t \geq 0. \tag{2.13}$$

Using the initial conditions in (2.7) and (2.13) we obtain the system of ordinary differential equations

$$\frac{ds}{dt} = -k_1 e_0 s + (k_1 s + k_{-1})c, \tag{2.14}$$

$$\frac{dc}{dt} = k_1 e_0 s - (k_1 s + k_{-1} + k_2)c, \tag{2.15}$$

with initial conditions

$$s(0) = s_0, \quad c(0) = 0. \tag{2.16}$$

The standard approach to solve these equations is to assume that at the initial stage of the reaction, formation of c is very fast and then after some time it reaches equilibrium, i.e.

$$\frac{dc}{dt} \approx 0. \tag{2.17}$$

Now, c can be expressed in terms of s from (2.15) as

$$c(t) = \frac{k_1 e_0 s(t)}{k_1 s(t) + k_{-1} + k_2}, \tag{2.18}$$

which implies

$$c(t) = \frac{e_0 s(t)}{s(t) + K_m}, \tag{2.19}$$

where

$$K_m = \frac{k_{-1} + k_2}{k_1} \tag{2.20}$$

is called the *Michaelis* constant. Here, even though the assumption is reasonable, the expression for $c(t)$ does not satisfy the initial condition in (2.16). However, in many real reactions this approximation is taken as a good approximation for $c(t)$. We therefore continue to solve for $s(t)$ by substituting (2.19) into (2.14) and we obtain

$$\begin{aligned} \frac{ds}{dt} &= -k_1 e_0 s + (k_1 s + k_{-1})\Big(\frac{e_0 s}{s + K_m}\Big), & (2.21) \\ &= \frac{-k_1 e_0 s^2 - k_1 e_0 K_m s + k_1 e_0 s^2 + k_{-1} e_0 s}{s + K_m}. & (2.22) \end{aligned}$$

Therefore

$$\frac{ds}{dt} = \frac{-k_2 e_0 s}{s + K_m}. \tag{2.23}$$

Now, using the initial condition $s(0) = s_0$ and (2.23) we can solve for $s(t)$ implicitly as

$$s(t) + K_m \log(s(t)) = s_0 + K_m \log(s_0) - k_2 e_0 t. \tag{2.24}$$

Substituting (2.24) into (2.19) we obtain an expression for the complex $c(t)$. Nonetheless this raises a few important questions: i) how fast is the initial transient; ii) for what range of the parameters does the approximation (2.19) and (2.24) hold; and iii) if the enzyme concentration is not small compared to the concentration of the substrate, how do we deal with it?

In fact, there are two types of time scales in this system: one is the initial transient timescale near $t = 0$ and the other is the longer time scale when the substrate changes significantly during which the approximations (2.19) and (2.24) are reasonable. To analyze this problem further, we need to nondimensionalise the system. To this end, we first introduce the concept of nondimensionalisation in the next section.

2.2 Nondimensionalisation

The form of a solution of a differential equation or a system of differential equations can depend critically on the units one chooses for the various quantities involved. These choices can lead to substantial problems when numerical approximation techniques such as Euler's method are applied. These difficulties can be controlled or overcome by a proper nondimensionalisation procedure [40].

Definition 2.2.1. Nondimensionalisation is the partial or the full removal of units from an equation involving physical quantities by suitable substitution of variables [40]. ■

Though there are no fixed steps to be followed to nondimensionalise a given system, the following steps are useful [40]:

1) Identify all the independent and dependent variables;

2) Replace each of them with a quantity scaled relative to a characteristic unit of measure to be determined;

3) Divide through by the coefficient of the highest order polynomial or by the coefficient of the highest order derivative term;

4) Choose the characteristic unit for each variable so that the coefficients of as many terms as possible become unity;

5) Rewrite the system of equations in terms of their new dimensionless quantities.

The last three steps are usually specific to the problem where nondimensionalisation is applied. However, almost all systems require the first two steps to be performed.

Example 2.2.2. Here we nondimensionalise the first order differential equation with constant coefficients [40, p 10]

$$a\frac{dx}{dt} + bx = Af(x). \tag{2.25}$$

In this equation the independent variable is t, and the dependent variable is x. Setting $x = \tilde{x}x_c$, $t = \tau t_c$, and then substituting these into (2.25) we obtain

$$a\frac{x_c}{t_c}\frac{d\tilde{x}}{d\tau} + bx_c\tilde{x} = Af(\tau t_c) = AF(\tau). \tag{2.26}$$

Now, dividing by the coefficient of the highest order derivative term, we obtain

$$\frac{d\tilde{x}}{d\tau} + \frac{bt_c}{a}\tilde{x} = \frac{At_c}{ax_c}F(\tau). \tag{2.27}$$

Thus, the coefficient of $\tilde{x}$ only contains one characteristic variable t_c, and hence it is easier to choose to set this to unity first as

$$\frac{bt_c}{a} = 1 \tag{2.28}$$

which implies

$$t_c = \frac{a}{b}. \tag{2.29}$$

Subsequently,

$$\frac{At_c}{ax_c} = \frac{A}{bx_c}, \tag{2.30}$$

which we set to unity to obtain

$$x_c = \frac{A}{b}. \tag{2.31}$$

Therefore, the final dimensionless equation in this case becomes completely independent of any parameters with units and is given by

$$\frac{d\tilde{x}}{d\tau} + \tilde{x} = F(\tau). \tag{2.32}$$

■

Example 2.2.3. We now consider a model of an outbreak of the Spruce budworm [25, p 7]

$$\frac{dp}{dt} = kp(1 - \frac{p}{N}) - \frac{Bp^2}{A^2 + p^2}, \quad p(0) = p_0. \tag{2.33}$$

We give a step by step approach to nondimensionalise this initial value problem. In this model p is the dependent and t is the independent variables. We take each variable and create a new variable by dividing the combination of parameters that has the same dimension in order to create a dimensionless variable. To this end, we set

$$u = \frac{p}{A}, \quad \tau = \frac{Bt}{A}, \tag{2.34}$$

and obtain

$$\frac{dp}{dt} = \frac{dp}{du}\frac{du}{d\tau}\frac{d\tau}{dt} = B\frac{du}{d\tau}. \tag{2.35}$$

Thus, substituting (2.34) and (2.35) into (2.33) and dividing both sides by B we obtain

$$\frac{du}{d\tau} = \frac{kA}{B}u\Big(1 - \frac{A}{N}u\Big) - \frac{u^2}{1+u^2}. \tag{2.36}$$

Introducing two new dimensionless parameters

$$\alpha = \frac{kA}{B}, \quad \beta = \frac{N}{A}, \tag{2.37}$$

we obtain

$$\frac{du}{d\tau} = \alpha u\Big(1 - \frac{u}{\beta}\Big) - \frac{u^2}{1+u^2}, \tag{2.38}$$

with $u(0) = \frac{p_0}{A}$. Thus, if we introduce another new parameter $\gamma = \frac{p_0}{A}$, then the initial condition becomes $u(0) = \gamma$.

Therefore, (2.33) has two dimensionless variables u, τ and three dimensionless parameters α, β, γ which are combinations of original parameters. This simplified form of the equation has reduced the number of parameters from five to three, which makes the analysis of the equation simpler. ■

Now, to analyze the quasi-steady state of the system (2.14)–(2.15), the standard way of nondimensionalising the system is to set

$$\tau = k_1 e_0 t, \quad u(\tau) = \frac{s(t)}{s_0}, \quad v(\tau) = \frac{c(t)}{e_0}, \tag{2.39}$$

and introducing new parameters by combining the original parameters as in (2.40)

$$\lambda = \frac{k_2}{k_1 s_0}, \quad k = \frac{k_2 + k_{-1}}{k_1 s_0} = \frac{k_m}{s_0}, \quad \epsilon = \frac{e_0}{s_0}, \tag{2.40}$$

which is a reasonable nondimensionalisation if $\epsilon \ll 1$. Substituting (2.39) and (2.40) into (2.14)–(2.15) together with (2.16) gives the dimensionless system

$$\frac{du}{d\tau} = -u + (u + k - \lambda)v, \tag{2.41}$$

$$\epsilon\frac{dv}{d\tau} = u - (u + k)v, \tag{2.42}$$

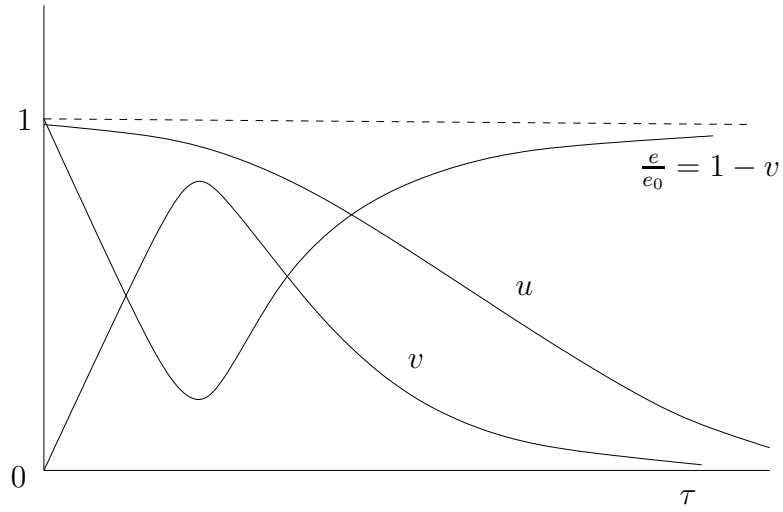

Figure 2.2: Schematic behavior of the solution of the system for dimensionless substrate (u), substrate-enzyme complex (v) and free enzyme ($e/e_0 = 1 - v$) concentrations as functions of dimensionless time τ [25].

with

$$u(0) = 1, \quad v(0) = 0. \tag{2.43}$$

With the solutions $u(\tau)$, $v(\tau)$ we immediately obtain e and p from (2.13) and (2.9) respectively. Moreover, from the reaction (2.1), which converts S into a product P, we obtain the steady state $u = 0$ and $v = 0$; that is, both the substrate and the substrate-enzyme complex concentrations are zero. We can also see that the time evolution of the nonlinear system (2.41)–(2.42) near $\tau = 0$ is governed by $\frac{du}{d\tau} < 0$ and $\frac{dv}{d\tau} > 0$ (because $v \approx 0$). As a result u decreases from $u = 1$ and v increases from $v = 0$ to $v = \frac{u}{u+k}$ (where $\frac{dv}{d\tau} = 0$). From (2.41), u is still decreasing at the point $v = \frac{u}{u+k}$. After v has reached its maximum then it decreases ultimately to zero as u does for all t. The dimensional enzyme concentration $e(t)$ first decreases from e_0 and then increases again to e_0 as $t \to \infty$. Typical solutions of the system (2.41)–(2.42) are illustrated in Figure 2.2.

2.3 Phase Diagrams and Linear Systems

In this section, we define the phase diagram and discuss some basic concepts pertinent to an analysis of linear systems.

2.3.1 Definitions

Consider a system of autonomous ordinary differential equations

$$\dot{\mathbf{x}} = \mathbf{f}(\mathbf{x}) \tag{2.44}$$

with $\mathbf{x} : \Re \to \Re^n$ and $\mathbf{f} : \Re^n \to \Re^n$. The space of all possible values of $\mathbf{x}$ is called the phase space of the system (2.44) [19].

In this brief introduction to the phase space, we shall only concentrate on the cases $\Re$ and $\Re^2$. In general, the phase space could be a subset of $\Re^n$, or a differentiable manifold. The velocity field $\mathbf{f}(\mathbf{x})$ is equal to the velocity $\dot{\mathbf{x}}$ of any solution curve $\mathbf{x}(t)$, and is therefore called the phase velocity vector field associated to the system (2.44). The trajectory of a solution $\mathbf{x}$ of (2.44) is the set of all points reached by $\mathbf{x}(t)$ for some value of t.

Definition 2.3.1. A phase diagram of (2.44) is the phase space $\Re^n$ with trajectories of (2.44) drawn through each point [19]. ■

Thus the phase diagram shows all the possible trajectories of an autonomous differential equation. However, in practice we only sketch a few trajectories. Points where the vector field $\mathbf{f}$ vanishes play an important role in understanding the qualitative behavior of solutions of the system (2.44).

Definition 2.3.2. An equilibrium point is a point where the vector field $\mathbf{f}$ vanishes [19]. ■

Note that every equilibrium point (also called fixed point or the steady state) $\mathbf{x}^*$ is itself a trajectory of a constant solution

$$\mathbf{x}(t) \equiv \mathbf{x}^* \tag{2.45}$$

since

$$\dot{\mathbf{x}} = \mathbf{f}(\mathbf{x}) = 0. \tag{2.46}$$

Definition 2.3.3. An equilibrium point $\mathbf{x}^*$ is called stable if for every $\epsilon > 0$ there exist a $\delta > 0$ so that [20]

$$|\mathbf{x_0} - \mathbf{x}^*| < \delta \Rightarrow |\mathbf{x}(t) - \mathbf{x}^*| < \epsilon, \quad t \geq 0 \tag{2.47}$$

for every solution $\mathbf{x}$ of (2.44) with $\mathbf{x}(0)$=$\mathbf{x_0}$. ■

Intuitively, an equilibrium point is called stable if, when we start close enough to it, we stay close to it. An equilibrium point is called unstable if it is not stable.

Definition 2.3.4. An equilibrium point $\mathbf{x}^*$ is called attracting if there is a $\delta > 0$ so that [20]

$$|\mathbf{x_0} - \mathbf{x}^*| < \delta \Rightarrow \mathbf{x}(t) \to \mathbf{x}^*, \quad \text{as} \quad t \to \infty \tag{2.48}$$

for every solution $\mathbf{x}$ of (2.44) with $\mathbf{x}(0)$=$\mathbf{x_0}$. ■

In one-dimensional systems attracting points are stable, but there exist attracting points which are not stable in higher dimensional systems.

Definition 2.3.5. An equilibrium point $\mathbf{x}^*$ is called asymptotically stable if it is stable and attracting [20]. ■

Example 2.3.6. Consider the equation [37, p 39]

$$\dot{x} = k_1 a x - k_2 x^2, \tag{2.49}$$

where k_1 and k_2 are positive rate constants and a and x are some chemical concentrations. The equilibrium points of (2.49) are obtained by setting

$$k_1 a x - k_2 x^2 = 0, \tag{2.50}$$

which implies

$$x = 0 \quad \text{or} \quad x = \frac{k_1 a}{k_2}. \tag{2.51}$$

To identify the stability of these equilibrium points, we sketch $\dot{x}$ versus x in Figure 2.3. Therefore, $x = 0$ is an unstable equilibrium point whereas $x = \frac{k_1 a}{k_2}$, which is positive, is a stable equilibrium point. ■

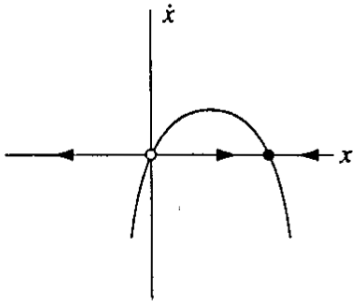

Figure 2.3: The phase diagram of the system (2.49).

2.3.2 Linear Systems

In this section, we briefly introduce linear homogeneous $n-$dimensional systems and then we investigate the properties of the equilibrium point using linear homogeneous two dimensional systems.

Consider a linear homogeneous system [19, p 164]

$$\dot{\mathbf{x}} = A\mathbf{x}, \tag{2.52}$$

where

$$\mathbf{x} = \begin{pmatrix} x_1 \\ x_2 \\ \vdots \\ x_n \end{pmatrix}, \tag{2.53}$$

and A is a real constant $n \times n$ matrix. Notice that $\mathbf{x} = \mathbf{0}$ is a solution of the system of differential equations (2.52). In fact, $\mathbf{x} = \mathbf{0}$ is the only equilibrium solution for the system where A is assumed to be a nonsingular matrix. The eigenvalues of the $n \times n$ matrix A are the roots of the characteristic polynomial

$$|A - \lambda I| = 0, \tag{2.54}$$

where I is the identity matrix of order n.

To explore the type of equilibrium points and their associated phase diagrams, we consider

linear homogeneous two dimensional systems

$$\frac{dx}{dt} = ax(t) + by(t), \tag{2.55}$$

$$\frac{dy}{dt} = cx(t) + dy(t), \tag{2.56}$$

which can be written in the form

$$\frac{d\mathbf{x}}{dt} = A\mathbf{x}(t), \tag{2.57}$$

with

$$A = \begin{pmatrix} a & b \\ c & d \end{pmatrix}. \tag{2.58}$$

Let λ_1 and λ_2 be the eigenvalues of the real matrix A defined in (2.58). Then, the general solution of (2.57) is

$$\begin{pmatrix} x \\ y \end{pmatrix} = c_1\mathbf{v_1}\exp(\lambda_1 t) + c_2\mathbf{v_2}\exp(\lambda_2 t), \tag{2.59}$$

where c_1 and c_2 are arbitrary constants and $\mathbf{v_1}$, $\mathbf{v_2}$ are eigenvectors of A corresponding to λ_1 and λ_2 respectively. We consider the different possibilities of λ_1 and λ_2 case by case as follows [20, p 226]:

Case 1: λ_1, λ_2 are real and distinct:

(a) $\lambda_1 < \lambda_2 < 0$: Suppose we have $c_1 > 0$, $c_2 = 0$. Then the trajectory corresponding to this solution will point along the ray in the direction of $\mathbf{v_1}$, with the arrow pointing towards to the origin. If $c_1 < 0$, $c_2 = 0$, the trajectory will point along the ray in the direction of $-\mathbf{v_1}$ with arrow pointing towards the origin. Similarly, if $c_1 = 0$, $c_2 > 0$ (< 0), the trajectory will point along the ray in the direction of $\mathbf{v_2}$, $(-\mathbf{v_2})$ with the arrow pointing towards to the origin. For $t \gg 0$ and both c_1 and c_2 different from zero, the $c_2\mathbf{v_2}\exp(\lambda_2 t)$ term will dominate and so the direction of approach to $(0, 0)$ will be parallel to the direction of $\mathbf{v_2}$. Similarly, when $t \to -\infty$ the first term $c_1\mathbf{v_1}\exp(\lambda_1 t)$ dominates, and the direction of the trajectory will approach that of $\mathbf{v_1}$. The phase diagram will have the form shown in Figure 2.4a. In this case the equilibrium point $(0, 0)$ is called a stable node.

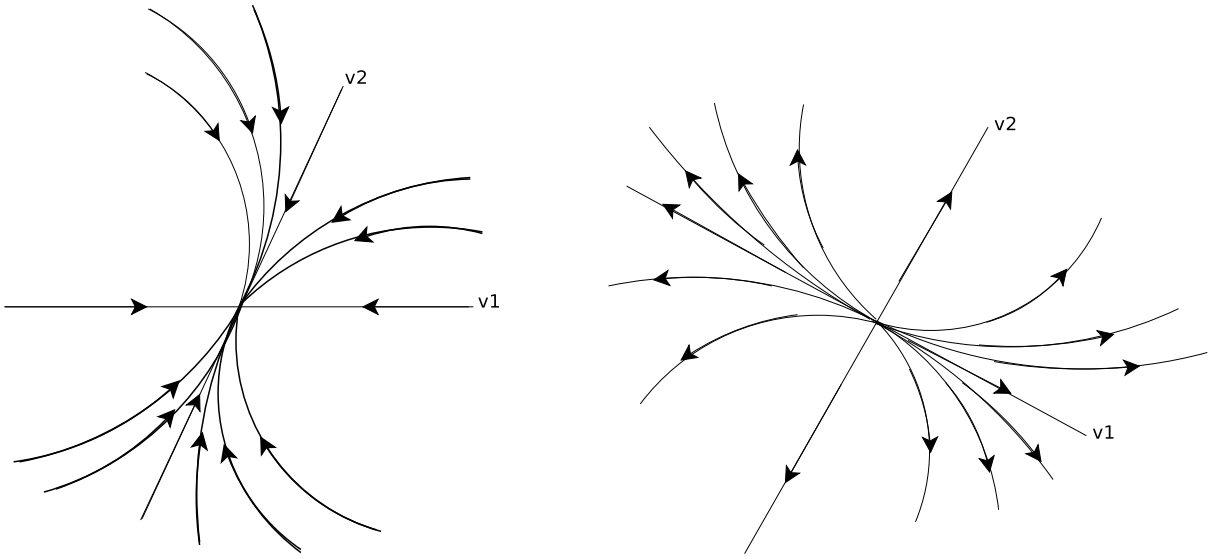

(a) Phase diagram when $\lambda_1 < \lambda_2 < 0$.

(b) Phase diagram when $0 < \lambda_1 < \lambda_2$.

Figure 2.4: Phase diagram of the system (2.57) for cases (a) and case (b).

(b) $0 < \lambda_1 < \lambda_2$: In this case all the trajectories will move out from the equilibrium point $(0, 0)$. As $t \to \infty$ the $c_2\mathbf{v_2}\exp(\lambda_2 t)$ term will dominate and so the direction of any trajectory will approach that of $\mathbf{v_2}$. As $t \to -\infty$ the $c_1\mathbf{v_1}\exp(\lambda_1 t)$ term will dominate and so the direction of any trajectory will approach that of $\mathbf{v_1}$. The phase diagram will have the form shown in Figure 2.4b. In this case the equilibrium point $(0, 0)$ is called unstable node.

Example 2.3.7. For the system [19, p 201]

$$\dot{x} = -2x + y, \tag{2.60}$$

$$\dot{y} = x - 2y, \tag{2.61}$$

$(0, 0)$ is the only equilibrium point. The system (2.60)–(2.61) can be rewritten as

$$\dot{\mathbf{x}} = \begin{pmatrix} -2 & 1 \\ 1 & -2 \end{pmatrix} \mathbf{x} = A\mathbf{x}. \tag{2.62}$$

λ is an eigenvalue of A if and only if

$$(-2 - \lambda)^2 - 1 = 0. \tag{2.63}$$

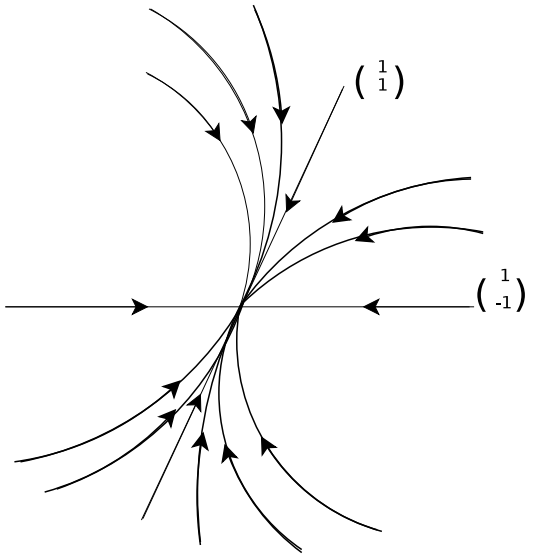

Figure 2.5: Phase diagram of the system (2.60)–(2.61).

Therefore, the eigenvalues are

$$\lambda_1 = -3 \quad \text{and} \quad \lambda_2 = -1. \tag{2.64}$$

Thus, $(0, 0)$ is a stable node. The eigenvectors corresponding to λ_1 and λ_2 are

$$v_1 = \begin{pmatrix} 1 \\ -1 \end{pmatrix} \quad \text{and} \quad v_2 = \begin{pmatrix} 1 \\ 1 \end{pmatrix}, \tag{2.65}$$

respectively. Therefore, the general solution is

$$\mathbf{x}(t) = c_1 \begin{pmatrix} 1 \\ -1 \end{pmatrix} \exp(-3t) + c_2 \begin{pmatrix} 1 \\ 1 \end{pmatrix} \exp(-t). \tag{2.66}$$

The phase diagram of the system (2.60)–(2.61) is shown in Figure 2.5. ■

(c) $\lambda_1 < 0 < \lambda_2$: In this case, if $c_1 = 0$, the trajectory is outward along the ray in the direction of $c_2\mathbf{v_2}$. If $c_2 = 0$, the trajectory is inward along the ray in the direction of $c_1\mathbf{v_1}$. As $t \to \infty$ the solution is dominated by $c_2\mathbf{v_2}\exp(\lambda_2 t)$ and when $t \to -\infty$ the solution is dominated by $c_1\mathbf{v_1}\exp(\lambda_1 t)$. Thus the phase diagram has the form shown in Figure 2.6. In this case the equilibrium point $(0, 0)$ is called a saddle point. It is always unstable (except strictly along $\mathbf{v_1}$) because any perturbation from $(0, 0)$ grows exponentially.

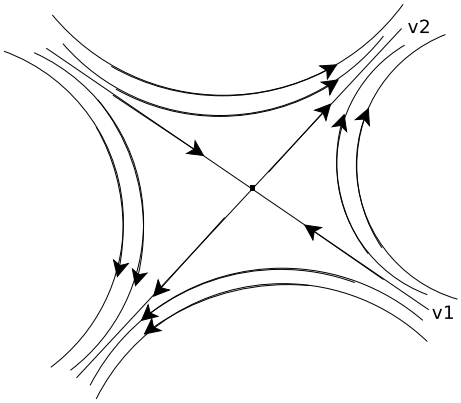

Figure 2.6: Phase diagram of the system (2.57) when $\lambda_1 < 0 < \lambda_2$.

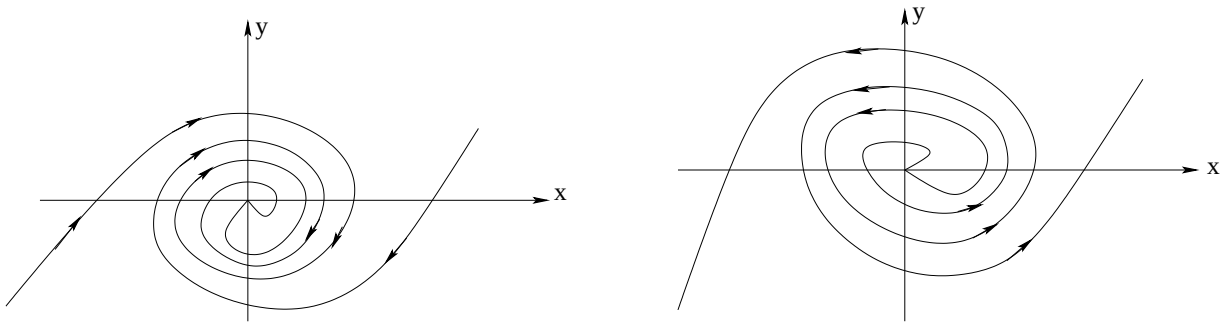

(a) Stable spiral

(b) Unstable spiral

Figure 2.7: Phase diagram of the system (2.57) when $\alpha \neq 0$.

Case 2: λ_1, λ_2 are complex: $\lambda_1 = \bar{\lambda}_2 = \alpha + i\beta$, $\beta \neq 0$.

In this case the general solution (2.59) involves $\exp(\alpha t)$ and $\exp(\pm i\beta t)$ which implies an oscillatory approach to $(0, 0)$.

(a) $\alpha \neq 0$: In this case we have a spiral which is stable if $\alpha < 0$ and unstable if $\alpha > 0$ (see Figure 2.7).

(b) $\alpha = 0$: In this case the phase curves are circles. This equilibrium point is called a centre and it is illustrated in Figure 2.8. The equilibrium point $(0, 0)$ is stable. However, since the trajectories stay at a fixed distance from the equilibrium point, it is not asymptotically stable.

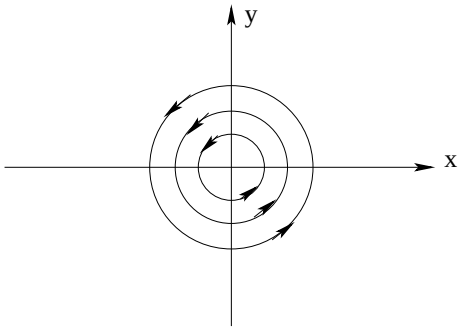

Figure 2.8: Phase diagram of the system (2.57) when $\alpha = 0$.

Example 2.3.8. For the system [19, p 203]

$$\dot{x} = x + y, \tag{2.67}$$

$$\dot{y} = 4x + y, \tag{2.68}$$

$(0, 0)$ is the only equilibrium point of the given system. Furthermore, the system (2.67)–(2.68) can be rewritten as

$$\dot{\mathbf{x}} = \begin{pmatrix} 1 & 1 \\ 4 & 1 \end{pmatrix} \mathbf{x} = A\mathbf{x}. \tag{2.69}$$

Then λ is eigenvalue of A if and only if

$$(1 - \lambda)^2 - 4 = 0. \tag{2.70}$$

Thus,

$$\lambda_1 = -1 \quad \text{and} \quad \lambda_2 = 3. \tag{2.71}$$

Eigenvectors corresponding to λ_1 and λ_2 are

$$v_1 = \begin{pmatrix} 1 \\ -2 \end{pmatrix} \quad \text{and} \quad v_2 = \begin{pmatrix} 1 \\ 2 \end{pmatrix}, \tag{2.72}$$

respectively. Thus the general solution is

$$\mathbf{x}(t) = c_1 \begin{pmatrix} 1 \\ -2 \end{pmatrix} \exp(-t) + c_2 \begin{pmatrix} 1 \\ 2 \end{pmatrix} \exp(3t). \tag{2.73}$$

The possible phase diagram of the system (2.67)–(2.68) is shown in Figure 2.9. ■

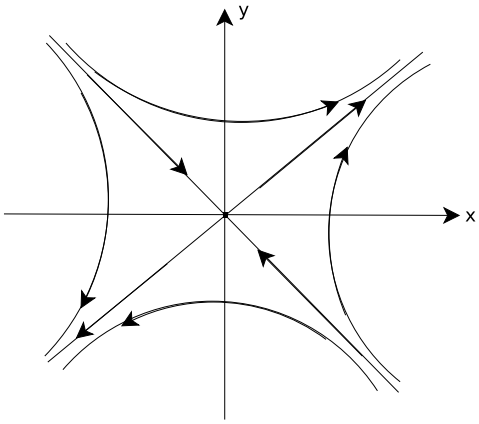

Figure 2.9: Phase diagram of the system (2.67)–(2.68).

2.4 Nonlinear Systems, Routh-Hurwitz and Bendixson Conditions

In this section, we first briefly introduce a nonlinear autonomous system of differential equations and discuss how to use the phase plane method to obtain qualitative information about the behaviour of a nonlinear system without actually solving the system. We then introduce Routh-Hurwitz conditions for stability of equilibrium points in higher dimensional space. We further discuss the Bendixson negative criterion for the existence of limit cycle solutions for the dynamical system in the specified domain.

2.4.1 Linearization

Consider a nonlinear system of differential equations

$$\dot{\mathbf{x}} = \mathbf{f}(\mathbf{x}), \tag{2.74}$$

where $\mathbf{f}$: $\Re^n \to \Re^n$ is nonlinear map and continuously differentiable on its domain. Such systems can not in general, be solved exactly. Hence, one can learn much about the qualitative behavior of the solutions by linearizing about the equilibrium points [20, p 219]. Unlike the linear homogeneous systems we discussed in section 2.3, the nonlinear autonomous system of

differential equations (2.74) may have several equilibrium points. We specifically discuss how to linearise the nonlinear system at the equilibrium point different from the origin later in our discussion in two dimensional space. We first focus on the linearisation of our system (2.74) about the equilibrium point

$$\mathbf{x}^* = \begin{pmatrix} x_1^* \\ x_2^* \\ \vdots \\ x_n^* \end{pmatrix}. \tag{2.75}$$

Let

$$\mathbf{x} = \mathbf{x}^* + \mathbf{h}, \tag{2.76}$$

where $\mathbf{h}$ is a small perturbation from the equilibrium point $\mathbf{x}^*$. Then we approximate $\mathbf{f}$ by the linear term in the Taylor expansion

$$\mathbf{f}(\mathbf{x}^* + \mathbf{h}) = \mathbf{f}(\mathbf{x}^*) + D\mathbf{f}(\mathbf{x}^*)\mathbf{h} + O(\mathbf{h}^2), \tag{2.77}$$

where $D\mathbf{f}(\mathbf{x}^*)$ is the Jacobian matrix evaluated at the steady state $\mathbf{x} = \mathbf{x}^*$ and $D\mathbf{f}$ is given by

$$D\mathbf{f} = \begin{pmatrix} \dfrac{\partial f_1}{\partial x_1} & \cdots & \dfrac{\partial f_1}{\partial x_n} \\ \vdots & & \vdots \\ \dfrac{\partial f_n}{\partial x_1} & \cdots & \dfrac{\partial f_n}{\partial x_n} \end{pmatrix}. \tag{2.78}$$

Since $\dot{\mathbf{h}} = \dot{\mathbf{x}} - \dot{\mathbf{x}}^* = \dot{\mathbf{x}}$, (2.74) has the linear approximation

$$\dot{\mathbf{h}} = D\mathbf{f}(\mathbf{x}^*)\mathbf{h}. \tag{2.79}$$

Thus, the nature of equilibrium points of a linear system of differential equations can be applied to equilibrium points in a nonlinear system.

We consider the following nonlinear system of differential equations in two dimensional space

$$\dot{x}(t) = f\big(x(t), y(t)\big), \tag{2.80}$$

$$\dot{y}(t) = g\big(x(t), y(t)\big), \tag{2.81}$$

where

$$\mathbf{x} = \begin{pmatrix} x \\ y \end{pmatrix}, \tag{2.82}$$

and f and g are smooth functions such that $f(a,b) = 0 = g(a,b)$ with (a,b) an equilibrium point. To linearize the system (2.80)–(2.81), we approximate the system close to the equilibrium point (a,b). Setting $x = a + \xi$, $y = b + \eta$ and taking a Taylor expansion of $f(x,y)$ and $g(x,y)$ we obtain

$$\begin{aligned} f(x,y) &= f(a,b) + \xi\frac{\partial f}{\partial x}(a,b) + \eta\frac{\partial f}{\partial y}(a,b) + \frac{1}{2!}\Big[\xi^2\frac{\partial^2 f}{\partial^2 x}(a,b) + 2\xi\eta\frac{\partial^2 f}{\partial x \partial y}(a,b) \\ &\quad + \eta^2\frac{\partial^2 f}{\partial^2 y}(a,b)\Big] + O(\xi^2,\eta^2), \\ &\approx \xi\frac{\partial f}{\partial x}(a,b) + \eta\frac{\partial f}{\partial y}(a,b), \end{aligned} \tag{2.83}$$

and similarly

$$g(x,y) \approx \xi\frac{\partial g}{\partial x}(a,b) + \eta\frac{\partial g}{\partial y}(a,b), \tag{2.84}$$

if ξ and η are very small. Noting that

$$\dot{x} = \dot{\xi} \quad \text{and} \quad \dot{y} = \dot{\eta}, \tag{2.85}$$

we deduce for (x,y) close to (a,b), the nonlinear system (2.80)–(2.81) is approximated by the linear system

$$\dot{\xi}(t) = \frac{\partial f}{\partial x}(a,b)\xi + \frac{\partial f}{\partial y}(a,b)\eta, \tag{2.86}$$

$$\dot{\eta}(t) = \frac{\partial g}{\partial x}(a,b)\xi + \frac{\partial g}{\partial y}(a,b)\eta. \tag{2.87}$$

The system (2.86)–(2.87) is called the linearized form of the system (2.80)–(2.81). The phase diagram of the linearized system close to $(0,0)$ gives a good approximation to the phase diagram of the nonlinear system. Furthermore, the solutions of the system (2.80)–(2.81) and the solutions of the system (2.86)–(2.87) behave similarly close to the equilibrium point (a,b).

Theorem 2.4.1. *(Linearization/Hartman-Grobman Theorem) [20] Let λ and μ be eigenvalues of*

$$\begin{pmatrix} \dfrac{\partial f}{\partial x} & \dfrac{\partial f}{\partial y} \\ \dfrac{\partial g}{\partial x} & \dfrac{\partial g}{\partial y} \end{pmatrix}(a,b). \tag{2.88}$$

If $Re(\lambda), Re(\mu) \neq 0$ and $\lambda \neq \mu$, then (a, b) is the same type of equilibrium point for both systems (2.80)–(2.81) and (2.86)–(2.87). ■

Possible types of equilibrium points are stable (or unstable) nodes, stable (or unstable) spirals, or saddle points.

Remark 2.4.2. For those cases which are not included in Theorem 2.4.1, we have the following remarks.

a) If $\lambda = i\omega$, then (a, b) is a centre for the linearised system but may become a stable or unstable spiral for the nonlinear system.

b) If $\lambda = \mu$ with $\lambda, \mu < 0$, then (a, b) is a stable improper node or stable star for the linearised system, but it may be either the same or a stable node or a stable spiral point for the nonlinear system.

c) If $\lambda = \mu$ with $\lambda, \mu > 0$, then (a, b) is unstable improper node or unstable star for the linearised system, but may be either the same or an unstable node or an unstable spiral point for the nonlinear system [20]. ■

Example 2.4.3. Consider the nonlinear system [19, p 206]

$$\dot{x} = 2y + xy, \tag{2.89}$$

$$\dot{y} = x + y. \tag{2.90}$$

The equilibrium points of the system (2.89)–(2.90) are $(0, 0)$ and $(-2, 2)$. The linearized system at $(0, 0)$ is

$$\dot{\mathbf{x}} = \begin{pmatrix} 0 & 2 \\ 1 & 1 \end{pmatrix} \mathbf{x} = A\mathbf{x}. \tag{2.91}$$

The eigenvalues of A are $\lambda_1 = -1$ and $\lambda_2 = 2$ with corresponding eigenvectors

$$v_1 = \begin{pmatrix} -2 \\ 1 \end{pmatrix} \quad \text{and} \quad v_2 = \begin{pmatrix} 1 \\ 1 \end{pmatrix}, \tag{2.92}$$

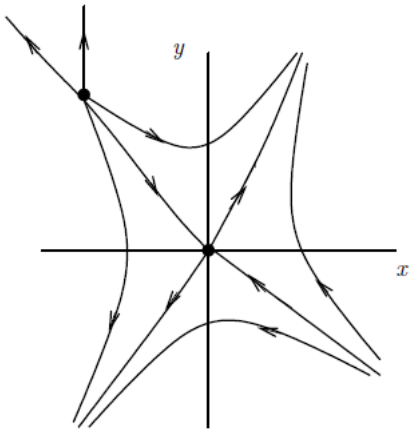

Figure 2.10: Phase diagram of the system (2.89)–(2.90).

respectively. Hence using Theorem 2.4.1, the equilibrium point $(0, 0)$ is a saddle point for both systems (2.89)–(2.90) and (2.91). The linearized system at $(-2, 2)$ is

$$\dot{\mathbf{x}} = \begin{pmatrix} 0 & 2 \\ 1 & 1 \end{pmatrix} \mathbf{x} = A\mathbf{x}. \tag{2.93}$$

The eigenvalues of A are $\lambda_1 = 1$ and $\lambda_2 = 2$ with corresponding eigenvectors

$$v_1 = \begin{pmatrix} 0 \\ 1 \end{pmatrix} \quad \text{and} \quad v_2 = \begin{pmatrix} 1 \\ 1 \end{pmatrix}, \tag{2.94}$$

respectively. Now using Theorem 2.4.1, $(-2, 2)$ is an unstable node for the system (2.93) and the system (2.89)–(2.89). A possible phase diagram for the system (2.89)–(2.90) is given in Figure 2.10.

2.4.2 Routh-Hurwitz Conditions and Bendixson Negative Criterion

Linear stability of the systems of ordinary differential equations which arise in reaction kinetics systems are determined by the nature of the roots of the characteristic polynomial. The stability analysis that we are concerned with involves systems of the form

$$\frac{d\mathbf{x}}{dt} = A\mathbf{x}, \tag{2.95}$$

where A is the matrix of the linearized form of the nonlinear reaction system. However, the techniques we developed so far are restricted only to 2-dimensional space systems. As a result, we further discuss the Routh-Hurwitz conditions for stability analysis in higher dimensional systems.

The Routh-Hurwitz conditions give the necessary and sufficient conditions for all roots of the characteristic polynomial (with real coefficients) to lie in the left half of the complex plane. These criteria are used to determine the asymptotic stability of the equilibrium point for a nonlinear system of differential equations. There are many equivalent forms of stating these criteria, one of which is stated in Theorem 2.4.4.

Theorem 2.4.4. *(Routh-Hurwitz Criteria) [12] Given the polynomial*

$$P(\lambda) = \lambda^n + a_1\lambda^{n-1} + \cdots + a_n,$$

where the coefficients $a_i, i = 0, 1, 2, \ldots n$ are real constants, define the n Hurwitz matrices as

$$H_1 = (a_1), \quad H_2 = \begin{pmatrix} a_1 & a_3 \\ 1 & a_2 \end{pmatrix}, \quad H_3 = \begin{pmatrix} a_1 & a_3 & a_5 \\ 1 & a_2 & a_4 \\ 0 & a_1 & a_3 \end{pmatrix}, \tag{2.96}$$

and

$$H_n = \begin{pmatrix} a_1 & a_3 & a_5 \ldots \\ 1 & a_2 & a_4 \ldots \\ 0 & a_1 & a_3 \ldots \\ \ldots & \ldots & \ldots \\ 0 & 0 & \ldots a_n \end{pmatrix}, \tag{2.97}$$

with $a_j = 0$ if $j > n$. All the roots of the polynomial $P(\lambda)$ are negative or have negative real parts if and only if the determinant of all Hurwitz matrices, denoted by

$$D_1 = a_1 > 0, \quad D_2 = \begin{vmatrix} a_1 & a_3 \\ 1 & a_2 \end{vmatrix} > 0, \quad D_3 = \begin{vmatrix} a_1 & a_3 & a_5 \\ 1 & a_2 & a_4 \\ 0 & a_1 & a_3 \end{vmatrix} > 0, \tag{2.98}$$

and

$$D_k = \begin{vmatrix} a_1 & a_3 & a_5 \dots \\ 1 & a_2 & a_4 \dots \\ 0 & a_1 & a_3 \dots \\ \dots & \dots & \dots \\ 0 & 0 & \dots a_k \end{vmatrix} > 0, \tag{2.99}$$

where $k = 1, 2, \dots, n$, *are positive.* ■

When $n = 2$, the Routh-Hurwitz criteria simplify to

$$D_1 = a_1 > 0, \quad D_2 = \begin{vmatrix} a_1 & 0 \\ 1 & a_2 \end{vmatrix} = a_1 a_2 > 0, \tag{2.100}$$

or equivalently $a_1 > 0$ and $a_2 > 0$. For characteristic polynomials of degree $n = 3, 4$ and 5, the Routh-Hurwitz criteria are summarized as

$$n = 3: \quad a_1 > 0, \quad a_3 > 0, \quad \text{and} \quad a_1 a_2 > a_3. \tag{2.101}$$

$$n = 4: \quad a_1 > 0, \quad a_3 > 0, \quad a_4 > 0, \quad \text{and} \quad a_1 a_2 a_3 > a_3^2 + a_1^2 a_4. \tag{2.102}$$

$$n = 5: \quad a_i > 0, \quad i = 1, 2, \dots, 5, \quad a_1 a_2 a_3 > a_3^2 + a_1^2 a_4, \quad \text{and}$$
$$(a_1 a_4 - a_5)(a_1 a_2 a_3 - a_3^2 - a_1^2 a_4) > a_5 (a_1 a_2 - a_3)^2 + a_1 a_5^2. \tag{2.103}$$

In the analysis of nonlinear systems, equilibrium points are not the only interesting points for which one may want to search. Limit cycles of the systems are also of interest.

Definition 2.4.5. A limit cycle is an isolated closed trajectory in the phase plane of the given system [19, 20, 37]. ■

If all neighbouring trajectories approach the limit cycle, we say the limit cycle is stable (Figure 2.11a); otherwise the limit cycle is unstable (Figure 2.11b), or in some cases, half-stable (Figure 2.11c). Stable limit cycles are very important scientifically– they model systems that exhibit self sustained oscillations. There are many examples that could be given, we mention only a few: the beating of the heart; daily rhythms in human body temperature and hormone secretion; and chemical reactions that oscillate spontaneously.

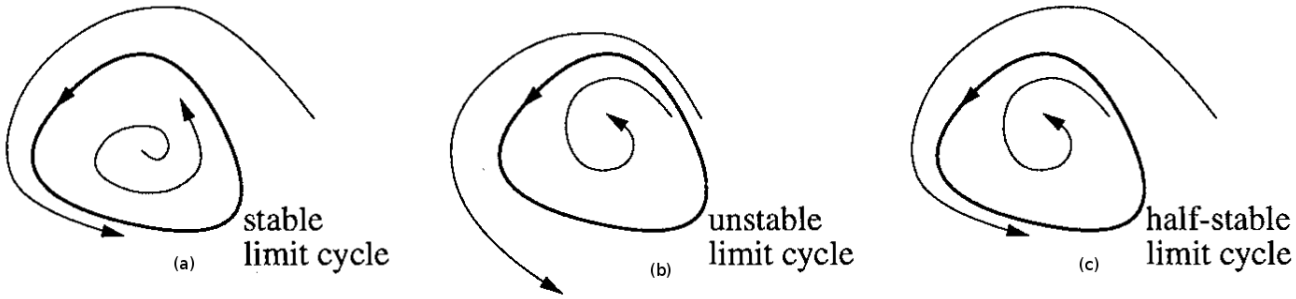

Figure 2.11: Different types of limit cycles.

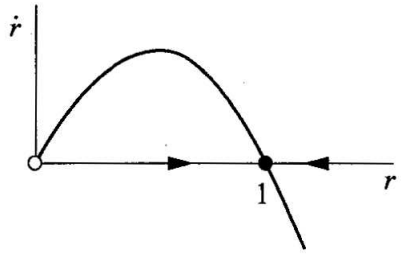

Figure 2.12: Equilibrium points and their stability nature of the system (2.104).

Example 2.4.6. Consider the system (in polar coordinate form) [37, p 143]

$$\dot{r} = r(1 - r^2), \tag{2.104}$$

$$\dot{\theta} = 1, \tag{2.105}$$

where $r \geq 0$. The radial and angular dynamics are uncoupled and so can be analyzed separately. From (2.104), we obtain $r = 0$ is an unstable equilibrium point and $r = 1$ is a stable as shown in Figure 2.12. Hence, in the phase plane, all trajectories (except $r = 0$) approach the unit circle $r = 1$ monotonically. Since the motion in the θ-direction is simply rotation at a constant angular velocity, we see that all trajectories spiral asymptotically toward the limit $r = 1$ as shown in Figure 2.13. ■

The criterion to identify the nonexistence of a limit cycle for a given dynamical system is stated as follows:

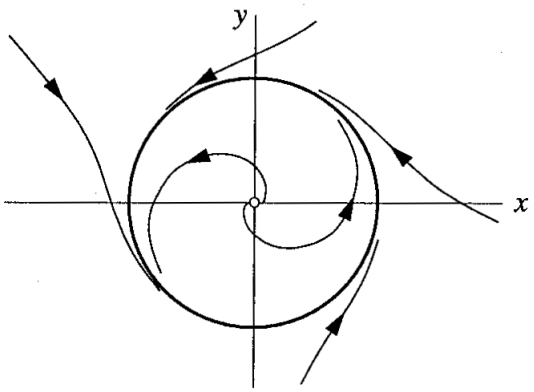

Figure 2.13: Limit Cycle of the system (2.104)–(2.105).

Theorem 2.4.7. *(Bendixson Negative Criterion) [20] Consider a nonlinear dynamical system*

$$\frac{dx}{dt} = F(x, y), \tag{2.106}$$

$$\frac{dy}{dt} = G(x, y), \tag{2.107}$$

where F and G are continuously differentiable functions on some simply connected domain, $D \subseteq \Re^2$. If

$$\bigtriangledown \cdot (F, G) = \frac{\partial F}{\partial x} + \frac{\partial G}{\partial y}, \tag{2.108}$$

is of one sign in D, there cannot be a limit cycle (closed orbit) contained within D. ■

Chapter 3

Mathematical Analysis of the Cancer Sub-Network Model

In this chapter, we discuss the formulation of the cancer subnetwork model, which is shown in Figure 1.4 and the nondimensionalization of the model. We further discuss the steady states and their stability behavior.

3.1 Key Assumptions

Based on the experimental evidence summarized in the introduction chapter, we make assumptions upon which our mathematical model is based in Table 3.1. Some assumptions are well grounded in the literature (such as assumptions $1-5$) while others remain to be tested.

3.2 Formulation of the Model

As we described in the introduction chapter, human cancers occur due to the dysfunction of some genes at the R-checkpoint during the cell cycle. Among these genes CycD, CycE, Cdk2, Cdk4, Cdk6, phosphatase Cdc25A, E2F, Rb, and $P27^{Kip1}$ are the key regulators in the control

Table 3.1: Key assumptions in our model

1	Constant stimulation rate of phosphatase Cdc25A and merging iCdc25A and aCdc25A	[3]
2	Constant stimulation rate of Cdk inhibitor P27^{Kip1}	[3, 36, 42]
3	Constant stimulation rate of CycE/Cdk2 and merging iCycE/Cdk2 and aCycE/Cdk2	[9, 42]
4	Mutual activation between Cdc25A and CycE/Cdk2	[2, 3, 34, 42]
5	Mutual inhibition between CycE/Cdk2 and P27^{Kip1}	[2, 3, 42] [9, 18, 36]
6	Only CycE/Cdk2 inhibits P27^{Kip1}	to be tested
7	First order degradation rates of Cdc25A, CycE/Cdk2, and P27^{Kip1}	to be tested
8	Negligible effect of multisite phosphorylation of Cdc25A and CycE/Cdk2	to be tested
9	Negligible effect of free and inactive form of CycE, Cdk2, and CycE/Cdk2	to be tested

of the G_1-to-S transition. It has been also experimentally shown that there is mutual activation between phosphatase Cdc25A and CycE/Cdk2 complex while mutual inhibition occurs between CycE/Cdk2 complex and Cdk inhibitor P27^{Kip1} [1, 2]. To understand the dynamics of these gene concentrations, a mathematical model of a hypothetical molecular mechanism for the regulation of CycE/Cdk2 activity, phosphatase Cdc25A and Cdk inhibitor P27^{Kip1} is developed as given in (3.3)–(3.5). This is done by translating the interaction mechanisms in Figure 1.4 into a set of autonomous nonlinear ordinary differential equations (ODEs) using the standard principles of biochemical kinetics [24, 38]. For the sake of simplicity we denote the concentration of each gene as $[Cdc25A] = x$, $[CycE/Cdk2] = y$, and $[P27^{Kip1}] = z$. We first discuss the nature of the degradation rate of the concentrations of the components. We assume each concentration degrades at a rate proportional to its concentration. For instance, the concentration of phosphatase Cdc25A degrades at a rate a proportional to its concentration given by

$$\frac{dx}{dt} = -ax, \tag{3.1}$$

as shown in Figure 3.1. We also assume the inhibition relationship between CycE/Cdk2 complex

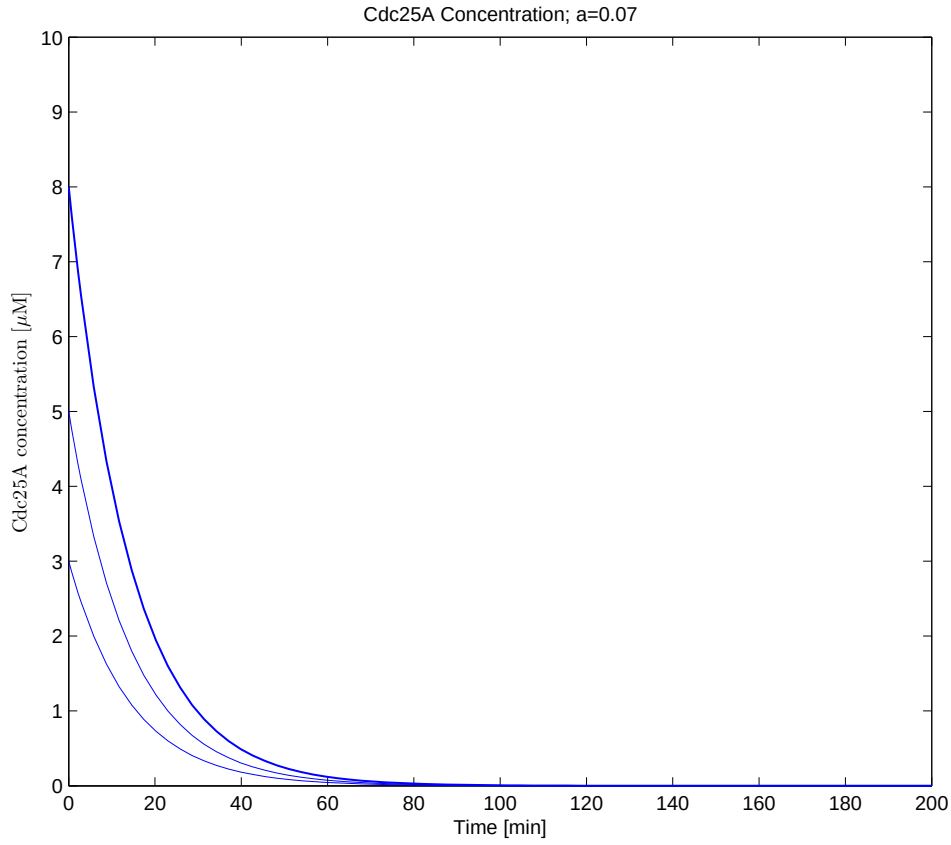

Figure 3.1: The degradation effect on the dynamics of Cdc25A with different initial conditions.

and CDK inhibitor $P27^{Kip1}$ can be expressed via a *Hill* function as defined in [33] as follows:

$$\frac{dy}{dt} = \frac{\rho k^n}{k^n + z^n} := h(z), \tag{3.2}$$

where k is the inhibition coefficient of z to y, and has units of concentration, ρ is production rate and n a parameter which measures the steepness of the function $h(z)$. In our study we will use the values ($\rho = 1\mu M/min$ and $n = 1$) unless otherwise indicated. Depending on the values of k and z, the dynamics of the CycE/Cdk2 complex could be different as shown in Figure 3.2. We then generate our cancer sub-network model as

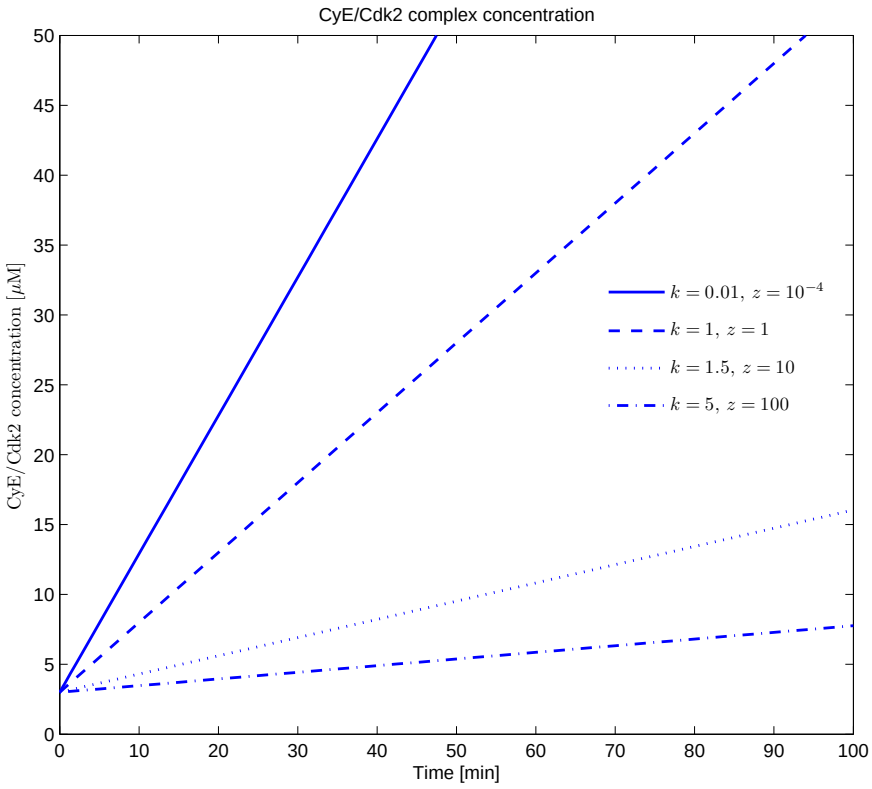

Figure 3.2: The inhibition effect on the dynamics of CyE/Cdk2 complex for different values of k and z.

$$\frac{dx}{dt} = \alpha + k_1 y - ax, \tag{3.3}$$

$$\frac{dy}{dt} = \beta + k_2 x - by + \frac{\rho k_3}{k_3 + z}, \tag{3.4}$$

$$\frac{dz}{dt} = \gamma - cz + \frac{\sigma k_4}{k_4 + y}, \tag{3.5}$$

where α and β are the constitutive protein expressions for the Cdc25A and CycE/Cdk2 complex due to signal transduction pathways stimulated by growth factors present in the extracellular medium (such as transcriptional factors E2F and C-Myc) respectively. The parameter γ represents the y independent constitutive transcription of z such as mitogenic signal stimulation. Parameters k_1 and k_2 are positive constant parameters which measure the efficiency of activation of y by x and x by y respectively (i.e. the mutual activation phenomenon). On the

other hand, k_3 and k_4 are positive inhibition coefficients and have unit of concentrations which measure the efficiency of the inhibition of z to y and y to z respectively (the mutual inhibition phenomenon) where as ρ and σ are the production rates of y by z and z by y respectively. For instance, the terms $\frac{\rho k_3}{k_3+z}$ and $\frac{\sigma k_4}{k_4+y}$ regulate the inhibition nature of z to y and y to z respectively, whereas the terms k_2x and k_1y are rates of x-induced transcription of y and y-induced transcription of x respectively. They are assumed to be first order in x and in y for the sake of simplicity; otherwise the transcription rate could be $\frac{\varphi x}{k_2+x}$ and $\frac{\phi y}{k_1+y}$, where φ and ϕ are production rates. The terms $-ax$, $-by$, and $-cz$ are a first order protein degradation with fixed rate coefficients a, b, and c due to ubiquitin-proteasome pathways.

3.3 Nondimensionalisation of the Model

Before analyzing the model, it is essential to express it in nondimensional terms. Doing so has some advantages. For example, the units used in the analysis are then unimportant and helps to reduce the number of parameters in dimensionless groups which determine the dynamics of the model. In any model there are usually different ways of nondimensionalisation possible and this model is no different. Consider the model (3.3)–(3.5) with nonnegative initial conditions

$$x(0) = x_0, \quad y(0) = y_0, \quad z(0) = z_0. \tag{3.6}$$

Setting

$$u(\tau) = \frac{k_2 x}{\beta}, \quad v(\tau) = \frac{k_1 y}{\alpha}, \quad w(\tau) = \frac{z}{k_3}, \quad \tau = ct, \tag{3.7}$$

we obtain

$$\frac{dx}{dt} = \left(\frac{\beta c}{k_2}\right)\left(\frac{du}{d\tau}\right), \quad \frac{dy}{dt} = \left(\frac{\alpha c}{k_1}\right)\left(\frac{dv}{d\tau}\right), \quad \text{and} \quad \frac{dz}{dt} = (ck_3)\left(\frac{dw}{d\tau}\right). \tag{3.8}$$

Substituting (3.7) and (3.8) into (3.3)–(3.5) we obtain

$$\frac{\beta c}{k_2}\frac{du}{d\tau} = \alpha + k_1\left(\frac{\alpha v}{k_1}\right) - a\left(\frac{\beta u}{k_2}\right), \tag{3.9}$$

$$\frac{\alpha c}{k_1}\frac{dv}{d\tau} = \beta + k_2\left(\frac{\beta u}{k_2}\right) - b\left(\frac{\alpha v}{k_1}\right) + \frac{\rho k_3}{k_3 + k_3 w}, \tag{3.10}$$

$$ck_3\frac{dw}{d\tau} = \gamma - ck_3 w + \frac{\sigma k_4}{k_4 + (\frac{\alpha v}{k_1})}. \tag{3.11}$$

Then (3.9)–(3.11) can be further simplified and give us

$$\frac{du}{d\tau} = \frac{\alpha k_2}{\beta c}(1+v) - \frac{a}{c}u, \tag{3.12}$$

$$\frac{dv}{d\tau} = \frac{\beta k_1}{\alpha c}(1+u) - \frac{b}{c}v + \frac{(\frac{\rho k_1}{\alpha c})}{1+w}, \tag{3.13}$$

$$\frac{dw}{d\tau} = \frac{\gamma}{ck_3} - w + \frac{(\frac{k_1 k_4}{\alpha})(\frac{\sigma}{ck_3})}{\frac{k_1 k_4}{\alpha} + v}. \tag{3.14}$$

Setting

$$\left(\frac{k_2}{\beta c}\right)\alpha = \alpha', \quad \left(\frac{k_1}{\alpha c}\right)\beta = \beta', \quad \left(\frac{1}{ck_3}\right)\gamma = \gamma', \quad \frac{\rho k_1}{\alpha c} = k_1',$$

$$\frac{a}{c} = a', \quad \frac{b}{c} = b', \quad \left(\frac{k_1}{\alpha}\right)k_4 = k_4', \quad k_4'\left(\frac{\sigma}{ck_3}\right) = q, \tag{3.15}$$

we obtain the nondimensionalised form of the model (3.3)–(3.5) as

$$\frac{du}{d\tau} = \alpha'(1+v) - a'u = f(u,v,w), \tag{3.16}$$

$$\frac{dv}{d\tau} = \beta'(1+u) - b'v + \frac{k_1'}{1+w} = g(u,v,w), \tag{3.17}$$

$$\frac{dw}{d\tau} = \gamma' - w + \frac{q}{k_4' + v} = h(u,v,w), \tag{3.18}$$

with nonnegative initial conditions $u(0) = u_0$, $v(0) = v_0$ and $w(0) = w_0$.

3.4 Steady State of the Model

The steady state(s), (u^*, v^*, w^*), are obtained by equating the right hand side of each equation (3.16)–(3.18) to zero. From (3.18) we obtain

$$w^* = \frac{\gamma' v^* + (\gamma' k_4' + q)}{v^* + k_4'}. \tag{3.19}$$

From (3.16) we obtain

$$u^* = \frac{\alpha' v^* + \alpha'}{a'}, \tag{3.20}$$

and then substituting (3.19) and (3.20) into (3.17) give us

$$\beta'(1 + \frac{\alpha' v^* + \alpha'}{a'}) - b' v^* + \frac{k_1'}{1 + (\frac{\gamma' v^* + (\gamma' k_4' + q)}{v^* + k_4'})} = 0, \tag{3.21}$$

or equivalently

$$\frac{(\beta' a' + \beta' \alpha') + \beta' \alpha' v^* - a' b' v^*}{a'} + \frac{k_1' v^* + k_1' k_4'}{(1+\gamma')v^* + (1+\gamma')k_4' + q} = 0, \tag{3.22}$$

which implies

$$[(1+\gamma')v^* + (k_4' + k_4'\gamma' + q)][(\alpha'\beta' - a'b')v^* + (\beta' a' + \beta'\alpha')] + a' k_1' v^* + a' k_1' k_4' = 0. \tag{3.23}$$

Thus

$$\begin{aligned}[(\alpha'\beta' - a'b')(1+\gamma')](v^*)^2 + [(k_4' + k_4'\gamma' + q)(\alpha'\beta' - a'b') + (\beta' a' + \beta'\alpha')(1+\gamma') \\ + a' k_1']v^* + (\beta' a' + \beta'\alpha')(k_4' + k_4'\gamma' + q) + a' k_1' k_4' = 0.\end{aligned} \tag{3.24}$$

Setting

$$k = (\alpha'\beta' - a'b')(1+\gamma'), \tag{3.25}$$

$$l = (\alpha'\beta' - a'b')(k_4' + k_4'\gamma' + q) + (\beta' a' + \beta'\alpha')(1+\gamma') + a' k_1', \tag{3.26}$$

$$m = (\beta' a' + \beta'\alpha')(k_4' + k_4'\gamma' + q) + a' k_1' k_4', \tag{3.27}$$

we can rewrite (3.24) as

$$k(v^*)^2 + l v^* + m = 0. \tag{3.28}$$

Since all the parameter values are positive (to be biologically meaningful), the constant term m in (3.28) is always positive. Hence the two solutions of (3.28) are given by

$$v_1^* = \frac{-l + \sqrt{l^2 - 4km}}{2k}, \tag{3.29}$$

and

$$v_2^* = \frac{-l - \sqrt{l^2 - 4km}}{2k}. \tag{3.30}$$

However, we are only interested in the positive solution of v^*. Thus we need to identify the condition(s) for which (3.28) has positive solutions. To do this we first calculate l^2 and $4km$:

$$\begin{aligned} l^2 &= [(\alpha'\beta' - a'b')(k_4' + k_4'\gamma' + q) + (\beta'a' + \beta'\alpha')(1+\gamma') + a'k_1']^2, \\ &= [(\alpha'\beta' - a'b')(k_4' + k_4'\gamma' + q)]^2 + [(\beta'a' + \beta'\alpha')(1+\gamma')]^2 + [a'k_1']^2 \\ &\quad + 2(\alpha'\beta' - a'b')(k_4' + k_4'\gamma' + q)(\beta'a' + \beta'\alpha')(1+\gamma') \\ &\quad + 2(\alpha'\beta' - a'b')(k_4' + k_4'\gamma' + q)(a'k_1') + 2(\beta'a' + \beta'\alpha')(1+\gamma')(a'k_1'), \end{aligned} \tag{3.31}$$

and

$$\begin{aligned} 4km &= 4[(\alpha'\beta' - a'b')(1+\gamma')][(\beta'a' + \beta'\alpha')(k_4' + k_4'\gamma' + q) + a'k_1'k_4'], \\ &= 4(\alpha'\beta' - a'b')(1+\gamma')(\beta'a' + \beta'\alpha')(k_4' + k_4'\gamma' + q) + 4(\alpha'\beta' - a'b')(1+\gamma') \\ &\quad (a'k_1'k_4'), \\ &= 4(\alpha'\beta' - a'b')(1+\gamma')(\beta'a' + \beta'\alpha')(k_4' + k_4'\gamma' + q) + 4(\alpha'\beta' - a'b')(k_4' + k_4'\gamma') \\ &\quad (a'k_1'). \end{aligned} \tag{3.32}$$

Then

$$\begin{aligned} l^2 - 4km &= [(\alpha'\beta' - a'b')(k_4' + k_4'\gamma' + q)]^2 + [(\beta'a' + \beta'\alpha')(1+\gamma')]^2 + [a'k_1']^2 \\ &\quad - 2(\alpha'\beta' - a'b')(1+\gamma')(\beta'a' + \beta'\alpha')(k_4' + k_4'\gamma' + q) \\ &\quad - 2(\alpha'\beta' - a'b')(k_4' + k_4'\gamma')a'k_1' + 2(\alpha'\beta' - a'b')(a'k_1'q) \\ &\quad + 2(\beta'a' + \beta'\alpha')(1+\gamma')(a'k_1'). \end{aligned} \tag{3.33}$$

By adding

$$2(\alpha'\beta' - a'b')(1+\gamma')(\beta'a' + \beta'\alpha')(k_4' + k_4'\gamma' + q), \tag{3.34}$$

and

$$2(\alpha'\beta' - a'b')(k_4' + k_4'\gamma' + q)(a'k_1'), \tag{3.35}$$

into (3.33) and subtracting the same term from it we obtain a new expression for $l^2 - 4km$ given by

$$l^2 - 4km = l^2 + 4(a'b' - \alpha'\beta')[\Delta], \tag{3.36}$$

where

$$\Delta = (k_4' + k_4'\gamma' + q)(\beta'a' + \beta'\alpha')(1 + \gamma') + (k_4' + k_4'\gamma')(a'k_1'), \tag{3.37}$$

which is always positive. Therefore, substituting (3.36) into (3.29) and (3.30) we obatin

$$v_1^* = \frac{-l + \sqrt{l^2 + 4(a'b' - \alpha'\beta')[\Delta]}}{2k}, \tag{3.38}$$

and

$$v_2^* = \frac{-l - \sqrt{l^2 + 4(a'b' - \alpha'\beta')[\Delta]}}{2k}. \tag{3.39}$$

For v^* to be a real solution,

$$l^2 + 4(a'b' - \alpha'\beta')[\Delta] \geq 0. \tag{3.40}$$

Furthermore, for v^* to be real and positive it also depends on the value of

$$a'b' - \alpha'\beta'. \tag{3.41}$$

We consider different cases to identify the condition(s) for the existence of positive values of v^*.

Case 1: $a'b' - \alpha'\beta' > 0$

This forces $k < 0$. Therefore, the only positive value of v^* is

$$v^* = \frac{-l - \sqrt{l^2 + 4(a'b' - \alpha'\beta')[\Delta]}}{2k}. \tag{3.42}$$

Case 2: $a'b' - \alpha'\beta' < 0$

This time $k > 0$. Therefore, there is no positive solution for v^*.

As a result we obtain

$$v^* = \frac{-l - \sqrt{l^2 + 4(a'b' - \alpha'\beta')[\Delta]}}{2k}, \tag{3.43}$$

as the only positive solution provided that

$$a'b' - \alpha'\beta' > 0. \tag{3.44}$$

To express this condition in terms of the original parameters, we use (3.15) and after substitution we obtain

$$a'b' - \alpha'\beta' = \frac{ab}{c^2} - \left(\frac{k_2}{\beta c}\right)\alpha\left(\frac{k_1}{\alpha c}\right)\beta > 0, \tag{3.45}$$

which implies

$$ab > k_1 k_2. \tag{3.46}$$

Therefore, the positive steady state(s), (u^*, v^*, w^*), can be calculated from

$$w^* = \frac{\gamma' v^* + (\gamma' k_4' + q)}{v^* + k_4'}, \tag{3.47}$$

$$u^* = \frac{\alpha' v^* + \alpha'}{a'}, \tag{3.48}$$

$$v^* = \frac{-l - \sqrt{l^2 + 4(a'b' - \alpha'\beta')[\Delta]}}{2k}, \tag{3.49}$$

where

$$a'b' - \alpha'\beta' > 0. \tag{3.50}$$

Theorem 3.4.1. *If $a'b' - \alpha'\beta' > 0$, then there is a positive steady state (u^*, v^*, w^*) given by (3.47)–(3.49) for all $\tau > 0$.*

Biologically, the condition $a'b' - \alpha'\beta' > 0$ (or equivalently $ab - k_1k_2 > 0$) means that the concentration of each component in the system (3.3)–(3.5) stabilizes at the positive values of (u^*, v^*, w^*) as given in (3.47)–(3.49) provided the combined degradation rate of Cdc25A and CycE/Cdk2 complex is greater than their combined activation rate. The model also produces

some of the fundamental features of CycE/Cdk2 complex and phosphatase Cdc25A. According to (3.48), the steady state of phosphatase Cdc25A and CycE/Cdk2 complex increases or decreases in the same direction. This model prediction agrees with the observations that the levels of Cdc25A and CycE are both increased in various tumors [8, 21, 39]. The model also clarifies the interpretation of Aguda and Tang [3], Kato [18], and Zhilin et al.[42] that an increase in CycE/Cdk2 level correlates with an increase in the level of Myc and E2F, both of which induce transcriptional signals to Cdc25A and results in promoting cell proliferation.

3.5 Stability Analysis of the Model

To determine the stability of the steady state (u^*, v^*, w^*), we need to calculate the eigenvalues of the Jacobian matrix of the system (3.16)–(3.18)

$$J = \left(\begin{array}{ccc} f_u & f_v & f_w \\ g_u & g_v & g_w \\ h_u & h_v & h_w \end{array} \right) \Bigg|_{(u,v,w)=(u^*,v^*,w^*)} \tag{3.51}$$

where

$$f_u = \frac{\partial f}{\partial u}. \tag{3.52}$$

Thus,

$$J = \left(\begin{array}{ccc} -a' & \alpha' & 0 \\ \beta' & -b' & \dfrac{-k_1'}{(1+w^*)^2} \\ 0 & \dfrac{-q}{(k_4'+v^*)^2} & -1 \end{array} \right). \tag{3.53}$$

The eigenvalue of the Jacobian matrix, J, is the value of λ such that

$$\left| \begin{array}{ccc} -a'-\lambda & \alpha' & 0 \\ \beta' & -b'-\lambda & \dfrac{-k_1'}{(1+w^*)^2} \\ 0 & \dfrac{-q}{(k_4'+v^*)^2} & -1-\lambda \end{array} \right| = 0. \tag{3.54}$$

This gives us

$$(-a'-\lambda)\Big[(-b'-\lambda)(-1-\lambda)-\frac{k_1'q}{(1+w^*)^2(k_4'+v^*)^2}\Big]-\alpha'\beta'(-1-\lambda)=0, \tag{3.55}$$

or equivalently

$$-\Big[a'\lambda^2+a'(b'+1)\lambda+a'b'-\frac{a'k_1'q}{(1+w^*)^2(k_4'+v^*)^2}+\lambda^3+(b'+1)\lambda^2+b'\lambda$$
$$-\frac{k_1'q\lambda}{(1+w^*)^2(k_4'+v^*)^2)}\Big]+\alpha'\beta'+\alpha'\beta'\lambda=0, \tag{3.56}$$

which implies

$$\lambda^3+(a'+b'+1)\lambda^2+\Big[b'+a'(b'+1)-\alpha'\beta'-\frac{k_1'q}{(1+w^*)^2(k_4'+v^*)^2}\Big]\lambda+a'b'-\alpha'\beta'$$
$$-\frac{a'k_1'q}{(1+w^*)^2(k_4'+v^*)^2}=0. \tag{3.57}$$

Setting

$$a_1 = a'+b'+1, \tag{3.58}$$

$$a_2 = b'+a'(b'+1)-\alpha'\beta'-\frac{k_1'q}{(1+w^*)^2(k_4'+v^*)^2}, \tag{3.59}$$

$$a_3 = a'b'-\alpha'\beta'-\frac{a'k_1'q}{(1+w^*)^2(k_4'+v^*)^2}, \tag{3.60}$$

we obtain the characteristic polynomial

$$\lambda^3+a_1\lambda^2+a_2\lambda+a_3=0. \tag{3.61}$$

To analyze the stability of the steady states (as our model is higher than 2-dimensional space), we use the Routh-Hurwitz conditions in the next section.

3.5.1 Asymptotic Stability

Using the Routh-Hurwitz conditions for stability, the steady state (u^*, v^*, w^*) is asymptotically stable (which means $Re(\lambda) < 0$ for all roots λ of (3.61)) if the following conditions are satisfied:

Condition 1:

$$D_1 = a_1 = a' + b' + 1 > 0, \tag{3.62}$$

(which is always true because all the terms in this expression are positive constants).

Condition 2:

$$D_2 = \begin{vmatrix} a_1 & a_3 \\ 1 & a_2 \end{vmatrix} > 0, \tag{3.63}$$

which implies

$$(a' + b' + 1)(b' + a'(b' + 1) - \alpha'\beta' - \frac{k_1' q}{(1 + w^*)^2(k_4' + v^*)^2}) - a'b' + \alpha'\beta' + \frac{a'k_1' q}{(1 + w^*)^2(k_4' + v^*)^2} > 0. \tag{3.64}$$

This can be written as

$$(a' + b' + 1)(a' + b') + (a' + b')(a'b') + (a' + b')(-\alpha'\beta') + \frac{(-b' - 1)k_1' q}{(1 + w^*)^2(k_4' + v^*)^2} > 0, \tag{3.65}$$

which is also equivalent to

$$(a' + b')(a' + b' + a'b' + 1) > (a' + b')(\alpha'\beta') + \frac{(b' + 1)k_1' q}{(1 + w^*)^2(k_4' + v^*)^2}, \tag{3.66}$$

and implies

$$(a' + b')(a' + b' + a'b' + 1) > (a' + b')(\alpha'\beta') + \frac{(b' + 1)k_1' q}{[(1 + \gamma')(k_4' + v^*) + q]^2}, \tag{3.67}$$

as

$$(1 + w^*)^2(k_4' + v^*)^2 = [(1 + \gamma')(k_4' + v^*) + q]^2. \tag{3.68}$$

Condition 3:

$$D_3 = a_3 > 0, \tag{3.69}$$

which implies

$$a'b' > \alpha'\beta' + \frac{a'k_1' q}{(1 + w^*)^2(k_4' + v^*)^2}, \tag{3.70}$$

or equivalently

$$a'b' > \alpha'\beta' + \frac{a'k_1'q}{[(1+\gamma')(k_4'+v^*)+q]^2}. \tag{3.71}$$

Therefore, for the steady state (u^*, v^*, w^*) to be asymptotically stable the conditions (3.62), (3.67) and (3.71) must hold.

3.5.2 Limit Cycles

Since periodicity is an inherent phenomenon in cell division cycle, we examine the existence of a limit cycle for our model using the Bendixson criterion. To this end, we take an arbitrary but fixed concentration of $P27^{Kip1}$, say P, and using (3.3)–(3.4) we obtain

$$\frac{dx}{dt} = \alpha + k_1 y - ax = F(x,y), \tag{3.72}$$

$$\frac{dy}{dt} = \beta + k_2 x - by + \frac{k_3}{k_3+P} = G(x,y). \tag{3.73}$$

Now, applying Theorem 2.4.7 we obtain

$$\frac{\partial F}{\partial x} + \frac{\partial G}{\partial y} = -(a+b) < 0, \tag{3.74}$$

for all $t > 0$.

Therefore, our model predicts that we cannot have a limit cycle solution for the molecular network containg CycE/Cdk2 complex and phosphatase Cdc25A if we keep the concentration of $P27^{Kip1}$ constant (which could be maintained by adjusting the mitogenic stimulation and the degradation rate of $P27^{Kip1}$).

Chapter 4

Numerical Simulations and Results of the Model

In this chapter, we discuss the various results we obtained from the mathematical analysis along with the numerical results. The ODEs in the model (3.3)–(3.5) are provided as input to *MatLab* [23] (a simulation software) using the package *Ode*45 to carry out the numerical simulations (refer to the appendix for the details of the MatLab code). Our results from the numerical simulations also confirm analyses in the literature. Many parameter values are obtained from the literature while a few are chosen by trial and error to fit the basic physiological behavior of the cell cycle process. However, in all our numerical simulation we use the value of $\rho = \sigma = 1\mu M/min$ unless otherwise indicated in the respective figure.

4.1 The Role of Phosphatase Cdc25A

Phosphatase Cdc25A is a key regulator of the G_1-to-S transition and is highly expressed in several types of cancers [21]. Overexpression of Cdc25A accelerates the G_1-to-S transition while its downregulation delays the G_1-to-S transition. In this section we examine only the dynamics of Cdc25A by keeping the concentration of the CycE/Cdk2 complex constant (because the

$P27^{Kip1}$ equation can be decoupled from the Cdc25A equation). We identify the important parameters that need to be controlled to keep the protein concentration of phosphatase Cdc25A at normal levels.

Using an arbitrary but fixed value of y, say K, and (3.3) we obtain the positive stable equilibrium point for Cdc25A

$$x^* = \frac{\alpha + k_1 K}{a}. \tag{4.1}$$

Since we assume that Cdc25A has only one phosphorylation site, regardless of the parameter choices the steady state is always stable as shown in Figure 4.1. This result agrees with the result of Zhilin et al. [42] under only one site for Cdc25A phosphorylation. The results in Figure 4.1 (a)-(d) show the effect of the Cdc25A degradation rate on the equilibrium point. As the degradation rate decreases, the value of the equilibrium point increases. Overexpression of phosphatase Cdc25A such as in Figure 4.1(d) leads to a quicker entry into S phase, geonomic instability, and tumorigenesis [21, 36, 42]. Our model also shows that downregulation of Cdc25A can be obtained by changing the synthesis rate, α, of Cdc25A as shown in Figure 4.2. To adjust the synthesis rate, α, one can adjust the concentrations of the transcriptional factors Myc and E2F using therapeutic drugs that target these transcription factors.

4.2 The Regulation of CycE/Cdk2 Complex

Proper CycE/Cdk2 regulation is important for the normal cell division cycle. Insufficient CycE/Cdk2 complex results in cell arrest in the G_1 phase, whereas overexpression of CycE/Cdk2 leads to premature entry into the S phase. When the CycE/Cdk2 expression increases, it may stay high. However, unless the concentration of CycE/Cdk2 is downregulated for normal DNA replication, the overexpression of CycE/Cdk2 (though it is stable) might be the cause for genomic instability and then for tumorigenesis [8, 18, 42]. The subnetwork in our model generates an abrupt change in the activity of CycE/Cdk2 for a certain choice of parameter values. In fact, the core of this sharp spike is the positive feedback loop between the Cdc25A and the CycE/Cdk2 complex, along with the mutual negative interaction between CycE/Cdk2 and

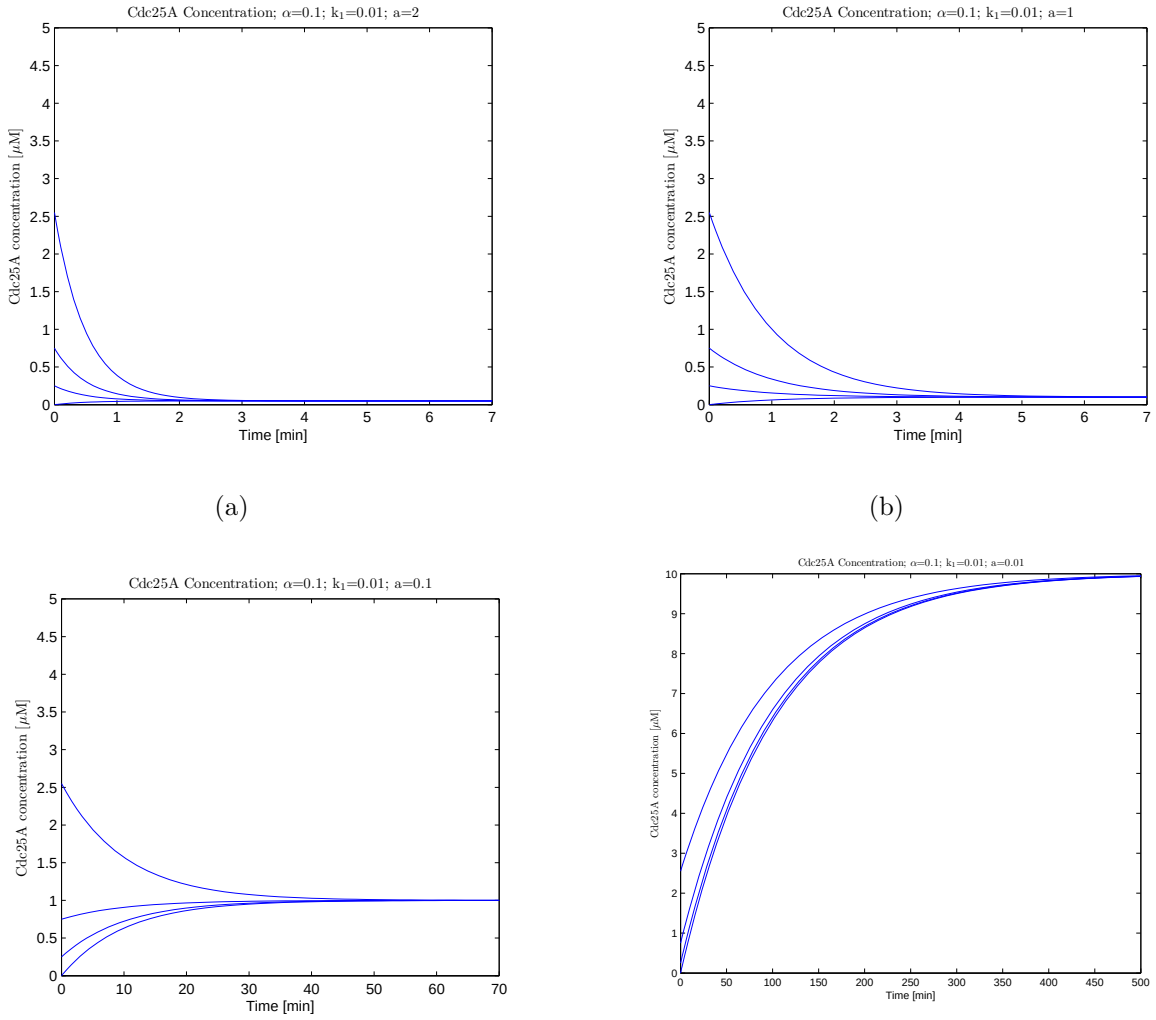

Figure 4.1: The effect of degradation rate on the dynamics of Cdc25A concentration taking $y = 10^{-6}$. In all cases, the solution curves converge to the equilibrium points. Equilibrium points: $x^* = 0.0500, 0.10000, 1.0000, 10.0000$ for Figures 4.1(a), (b), (c), and (d) respectively. Initial Conditions: $x(0) = 2 \times 10^{-5}$, 0.25, 0.75, 2.55.

$P27^{Kip1}$ as shown in Figure 4.3. A distinctly sharp pulse of CycE/Cdk2 activity is generated at lower levels of $P27^{Kip1}$ and then regulated by the higher level of $P27^{Kip1}$ which confirms the results in [3, 18, 42]. We further examine the dynamics of CycE/Cdk2 and $P27^{Kip1}$ by keeping Cdc25A constant. The timing of the increase in CycE/Cdk2 activity coincides with the decay of $P27^{Kip1}$ as shown in Figure 4.4. Our simulation result agrees with the results of Aguda and

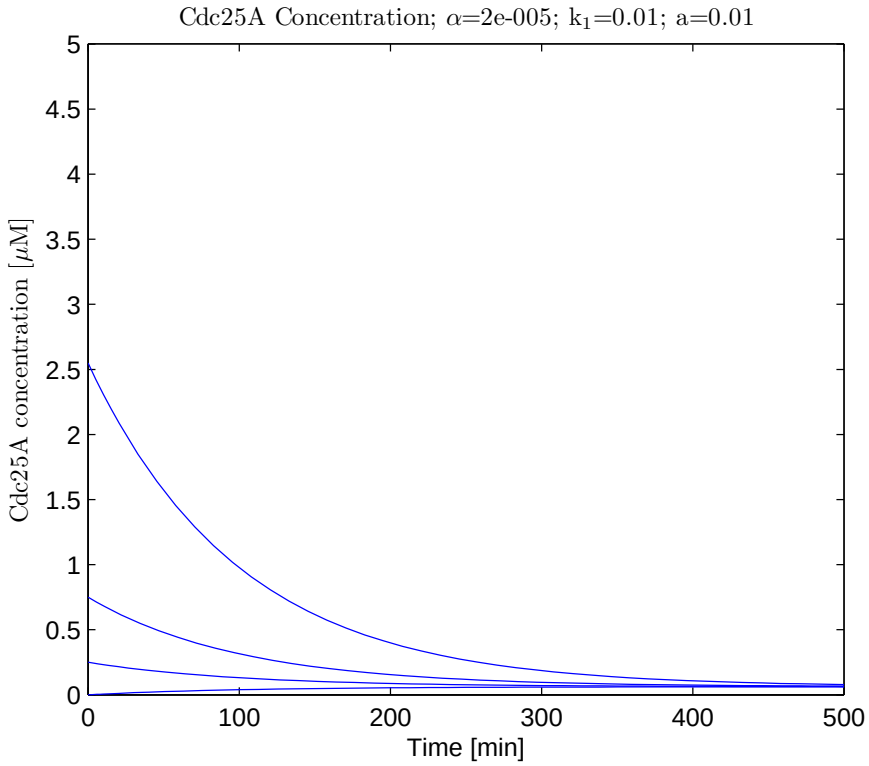

Figure 4.2: The effect of synthesis rate of Cdc25A on the value of equilibrium point. Initial values: $x(0) = 2 \times 10^{-5}$, 0.25, 0.75, 2.55, and $y = 0.06$. Equilibrium point: $x^* = 0.0620$

Tang [3] and Zhilin et al. [42].

4.3 The role of P27^{Kip1}

Generating a pulse of CycE/Cdk2 activity before the S phase entry requires more components of the network in Figure 1.3 to be included as well as choosing appropriate parameter values (especially for CycE and E2F degradation rates) which will affect the Cdc25A degradation rate. However, in our model, the cancer subnetwork (Figure 1.4) and the nonlinear system of differential equations (3.3)–(3.5) are used to carry out a series of simulations to see the effect of different levels of P27^{Kip1}. The results are shown in Figure 4.5. The simulations show that the initial P27^{Kip1} level influences the switch on time (the time required by the CycE/Cdk2 solution

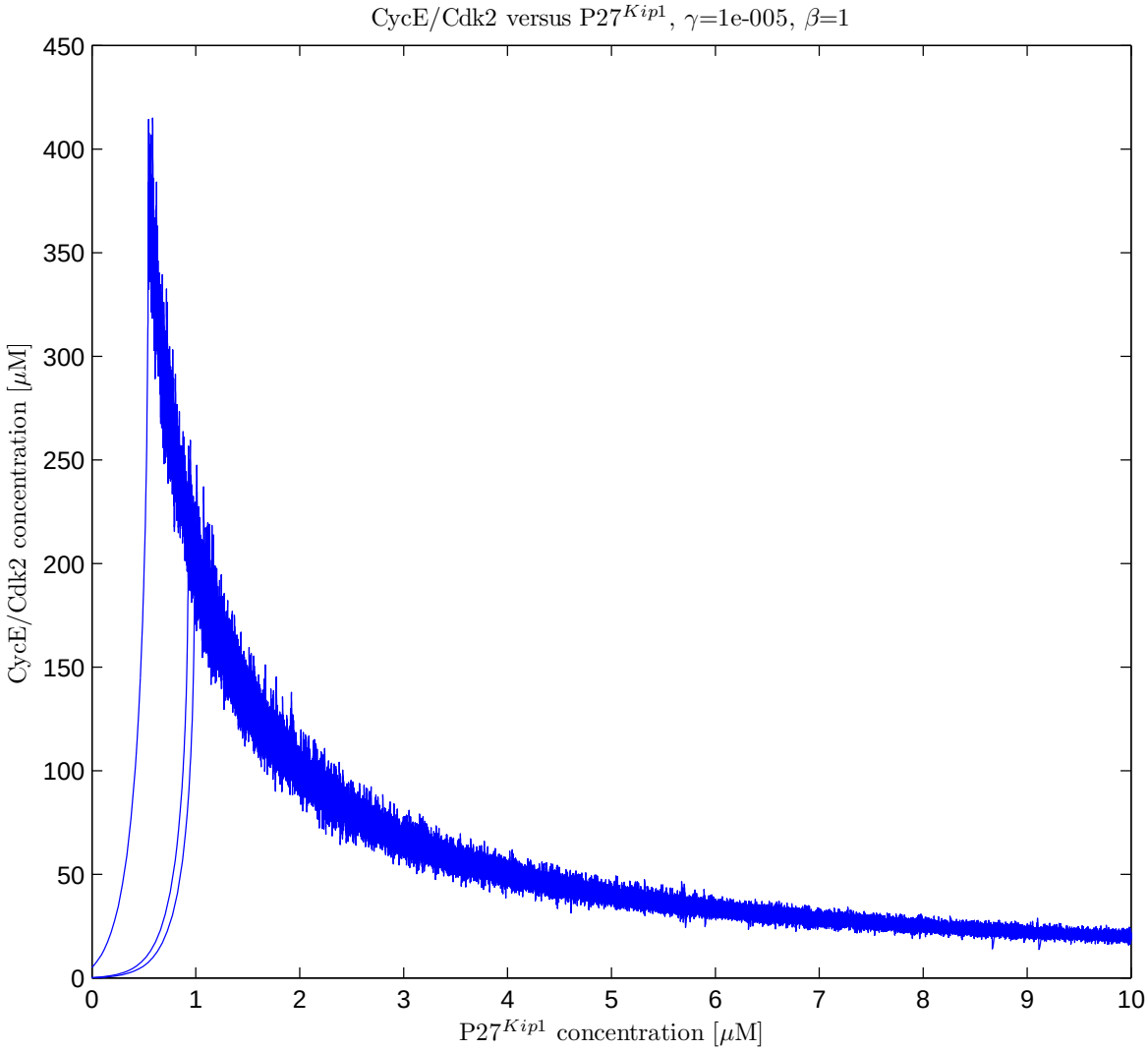

Figure 4.3: The effect of constantly stimulating P27^{Kip1} on the dynamics of CycE/Cdk2 with different initial conditions. Initial conditions: $y(0) = 10^{-6}$, 0.1, 5 and $x = 2 \times 10^{-5}$. Parameter values: $k_2 = 0.2$, $k_3 = 0.1$, $k_4 = 0.2$, $b = 0.001$, $c = 0.001$.

curve to cross and to remain above the solution curve of P27^{Kip1}) for CycE/Cdk2 activity. The lower the P27^{Kip1} level, the shorter the time needed to activate CycE/Cdk2. However, in this particular simulation we also observed that Cdc25A and CycE/Cdk2 complex seem increasing indefinitely as long as we keep P27^{Kip1} level below some threshold value.

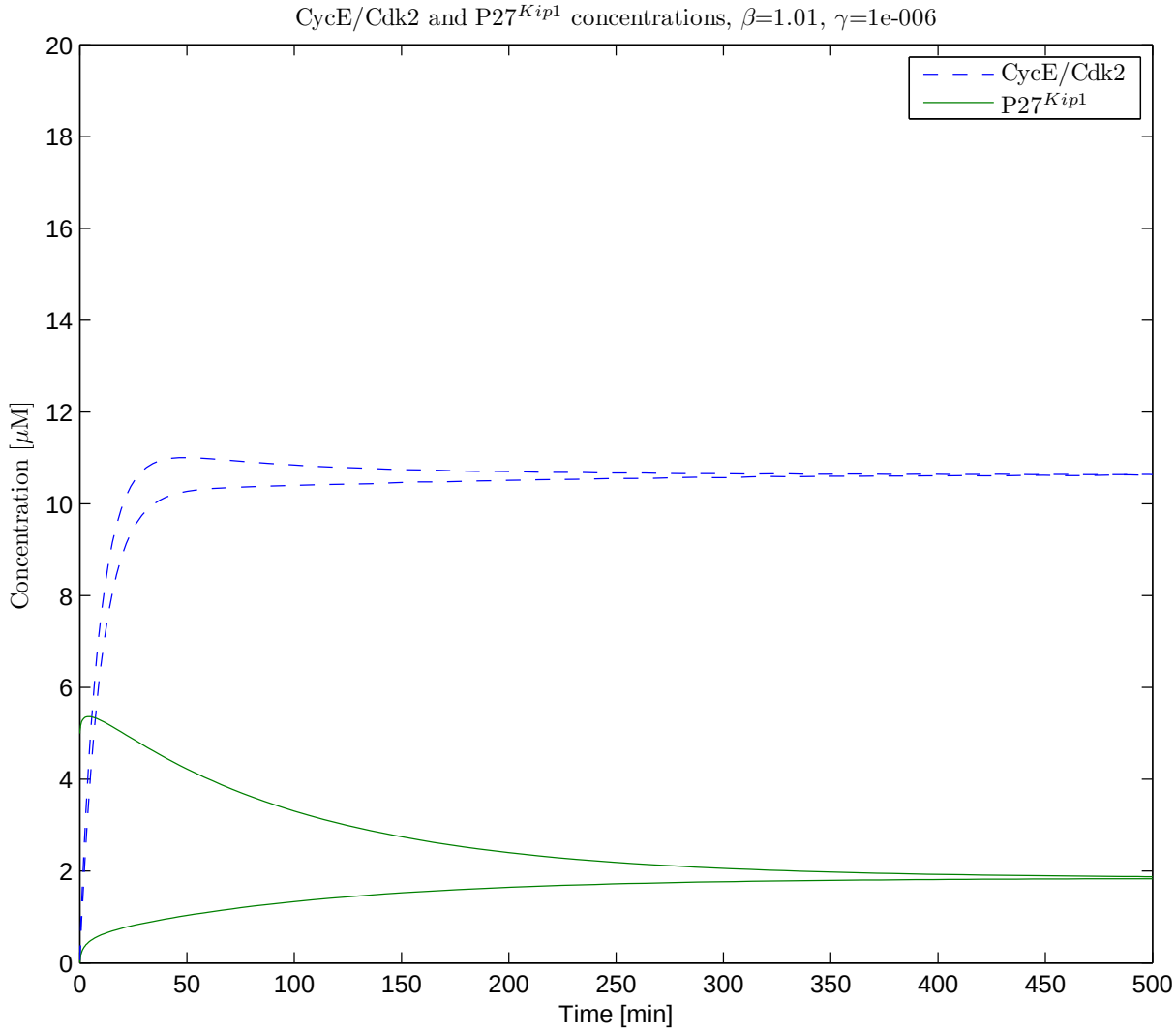

Figure 4.4: The effects of P27^{Kip1} on the peak activity of CycE/Cdk2 with different initial conditions. $y(0) = 0.06$, $z(0) = 10^{-6}$, 5, $x = 0.01$. Parameter values: $k_2 = 0.2$, $k_3 = 0.1$, $k_4 = 0.2$, $b = 0.1$, $c = 0.01$.

In this simulation, the positive feedback loop between CycE/Cdk2 and Cdc25A is also reflected. When the concentration level of CycE/Cdk2 rises (because of the lower level of P27^{Kip1}), the concentration level of phosphatase Cdc25A starts to rise and requires a shorter time to reach the switch on time.

4.4 The Dynamics of the Model

In the simulation of the model that takes into account all the molecular concentrations of Cdc25A, CycE/Cdk2 and $P27^{Kip1}$, we obtain results that support our analytical solutions. In this simulation, as long as we keep the condition (3.46) (which is the condition for the existence of a positive equilibrium point as shown (3.47)–(3.49)), all the solution curves converge to the equilibrium point (Figures 4.6a–b). Moreover, our model shows that the downregulation of $P27^{Kip1}$ can be achieved through either cutting off (reducing) the mitogenic stimulation of $P27^{Kip1}$ or increasing its degradation rate (Figure 4.6b). In these simulations (Figures 4.6a–b), even though we have three different initial conditions for each concentration, the solution curves of CycE/Cdk2 complex and Cdc25A coincides immediately from the beginning. Moreover, in Figure 4.6b the concentration of $P27^{Kip1}$ is almost identical to zero ($z^* = 0.0198$).

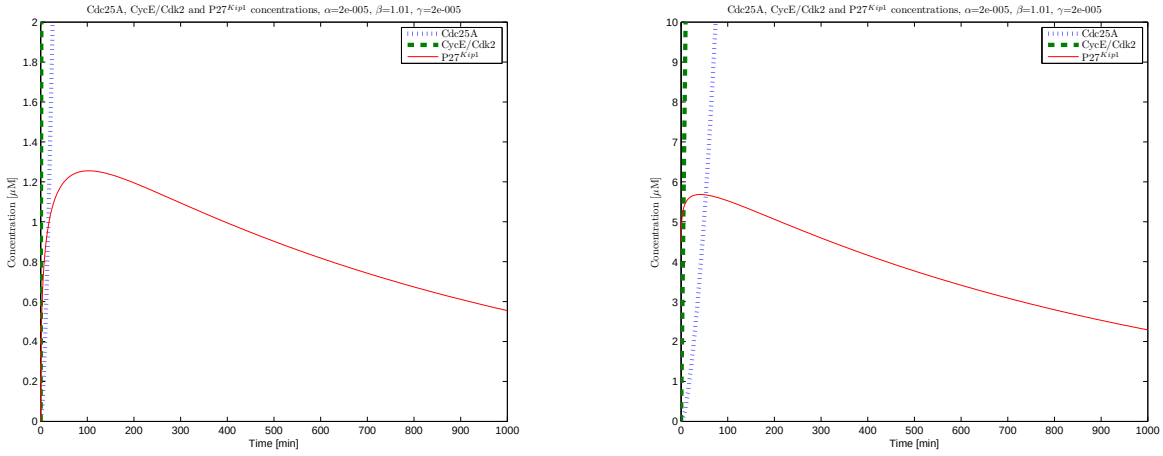

(a)

(b)

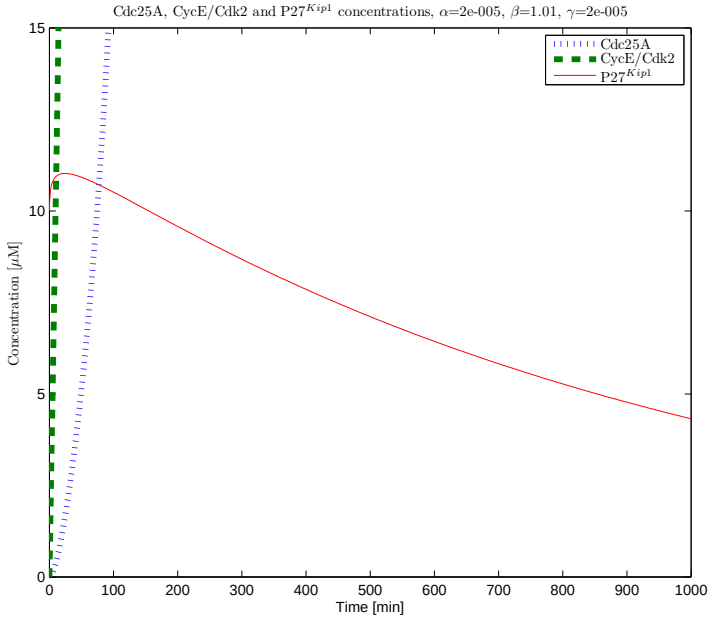

(c)

Figure 4.5: The effect of $P27^{Kip1}$ levels on the activity of Cdc25A and CycE/Cdk2. Initial levels of $P27^{Kip1}$: a) 10^{-3} b) 4.5 c) 10. Parameter values: $k_1 = 0.01$, $a = 0.1$, $k_2 = 0.2$, $b = 0.002$, $k_3 = 0.1$, $c = 10^{-3}$, $k_4 = 0.3$. Initial conditions: $x = 0.01$, $y = 10^{-4}$.

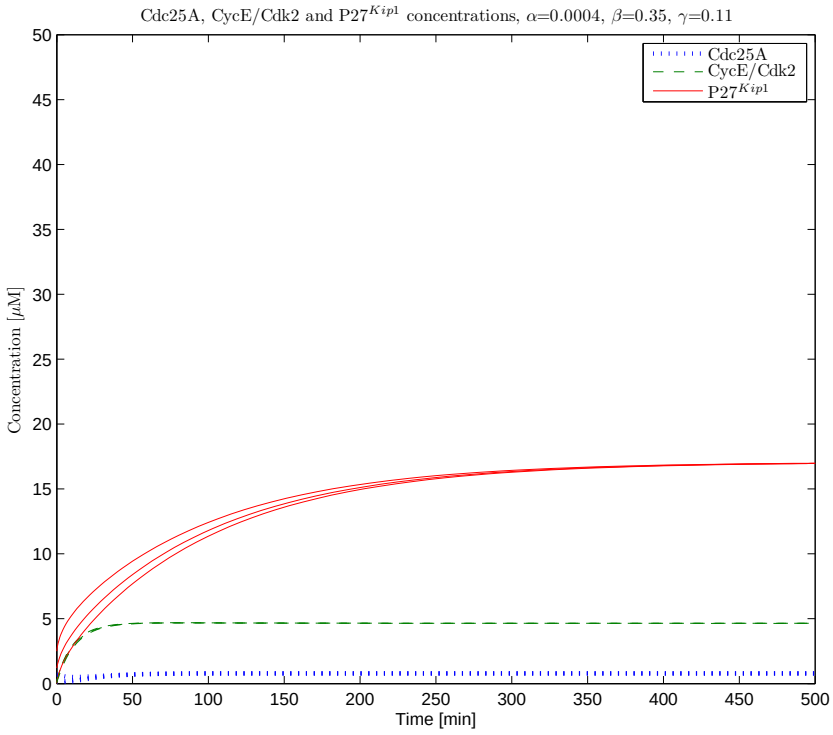

(a) Parameter value: $c = 10^{-2}$

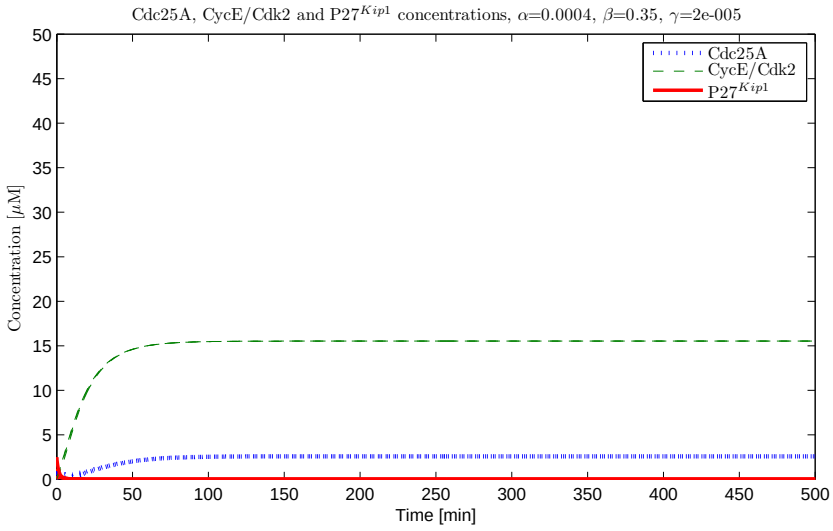

(b) Parameter value: $c = 1$

Figure 4.6: Model dynamics for different initial conditions. Common parameter values for (a) and (b): $k_1 = 0.01$, $a = 0.06$, $k_2 = 0.02$, $b = 0.08$, $k_3 = 0.1$, $k_4 = 0.3$. Initial conditions: $(x(0), y(0), z(0))$=$(10^{-2}, 10^{-5}, 10^{-3})$, $(0.02, 0.06, 1.2)$,$(0.7, 0.27, 2.5)$. Equilibrium points: $(x^*, y^*, z^*) = (0.7841, 4.6550, 16.2100)$ and $(2.4040, 15.4410, 0.0198)$ for Figures 4.6(a) and (b) respectively.

Chapter 5

Conclusions

5.1 Summary of the Results

The cancer subnetwork presented in our study is grossly simplified from what is currently known about the molecular and the gene interactions of oncogenes and tumor suppressor genes. However, the full cancer network during the cell cycle process is too complex to be modeled computationally at once. To model the cancer network we started with a simple model that captured the basic features of the network. This model can be later made more realistic.

In this study, a core cancer subnetwork consisting of Cdc25A, CycE/Cdk2 complex and $P27^{Kip1}$ was identified and a new mathematical model was also developed. Mathematical analyses and numerical simulations were carried out and the results are consistent with various results in the literature. One of the aims of this study was to see whether there is a critical parameter of this subnetwork which is responsible for the sudden increase of the CycE/Cdk2 complex concentration. Indeed, our model simulation result showed that (keeping the other parameter values fixed) the subnetwork generates a peak value of CycE/Cdk2 activity when the degradation rate of the complex is generally less than 0.001 min^{-1} (Figure 4.3). Our model results also suggest that CycE/Cdk2 regulates $P27^{Kip1}$. The CycE/Cdk2 activity reverses the inhibitory effect that $P27^{Kip1}$ has on cell cycle progression at the R checkpoint and initiates a pathway

that leads to the elimination of $P27^{Kip1}$ from the cell (Figure 4.6b). On the other hand, we also show that the downregulation of $P27^{Kip1}$ is prevented by decreasing the catalytic activity of the CycE/Cdk2 complex which could be adjusted by changing the E2F transcription rate, by increasing the degradation rate of CycE/Cdk2 or by decreasing the constant simulation rates of Cdc25A and CycE/Cdk2 (Figure 4.6a). A recent study [42] showed that the failure to degrade CycE stabilized the CycE/Cdk2 complex at high level which led to tumorigenesis, similar to the overexpression of Cdc25A. The regulation of CycE/Cdk2 is essential to prevent cells from becoming cancerous. Our model results show that the high degradation rate of CycE/Cdk2 makes the concentration of CycE/Cdk2 very low and a low degradation rate keeps the concentration of CycE/Cdk2 complex high. This could be taken as a therapeutic target gene for cancer treatment.

Phosphatase Cdc25A promotes cell cycle progression and is overexpressed in numerous rapidly dividing cancer cells. An increasing number of studies have shown a positive correlation between overexpression of Cdc25A and cancer [21, 29]. Our model results also suggest that the overexpression of Cdc25A leads to the increase in the activity of CycE/Cdk2 (Figure 4.6b) which subsequently lead to an uncontrolled proliferation of cells.

5.2 Remarks and Future Work

Although our results are consistent with many experimental results and confirm results from the literature, there are some limitations in our study. The first limitation is that no clear data on the rate parameters are available which makes the investigation of the numerical simulation difficult. Secondly, there are more regulatory interaction components such as PRb, E2F family, CycD/Cdk4 and their multisite phosphorylation properties which highly influence the activity of Cdc25A and CycE/Cdk2 complex. These were not incorporated directly into our model. Nevertheless, we obtained promising results that motivate us to modify our model so as to further explore the dynamics of the cell cycle and to identify some therapeutic strategy to treat cancer.

In our model, we used linear degradation terms. We wish to modify these terms of our model using functions such as

$$\frac{-ax}{A+x}, \quad \frac{-bx}{B+y}, \quad \frac{-cx}{C+z}, \tag{5.1}$$

which may express the real biological protein concentration degradation phenomenon more accurately. We also used a reciprocal function to express the inhibition relationship between CycE/Cdk2 and $P27^{Kip1}$. It is our intention to modify the inhibition relationship using a function of the form

$$\frac{k}{q+z^m}, \tag{5.2}$$

where k, q and m are *Hill* coefficients [33]. We hope the oscillatory nature of the solution can be achieved by choosing an appropriate value of the Hill exponent m along with adding some more key regulatory components (such as PRb, E2F, and/or the INK4 CDK inhibitor family) into our cancer sub-network. This is the subject of future work.

Appendix A

MatLab Codes Used in our Numerical Simulations

A.1 The Dynamics of Phosphotase Cdc25A

```
 This MatLab code illustrates the evolution of the phosphotase Cdc25A concentration
 keeping CycE/Cdk2 constant.
Clear up the previous definitions.
clear all;
close all;
Codes that define the input parameters.
%%tmax=input(tmax);
%%alpha=input(alpha);
%%k1=input(k1);
%%a=input(a);
Codes that solve the system numerically using the package Ode45.
%%disp('The problem is being solved using ode45...')
%%[tt,xx]=ode45(@(t,x)cdc25a,[tmin,tmax],initial conditions);
Codes that solve the system graphically.
```

```
%%disp('plotting solution is being carried out...')
%%plot(tt,xx(:,1))
Codes that describe the graphical solution.
%%title_cdc25a=['Cdc25A Concentration; $\alpha$=',num2str(alpha),';
%%k$_{1}$=',num2str(k1),'; a=',num2str(a)];
%%title(title_cdc25a)
Codes that label axes and produce multiple plots.
%%xlabel(Time [min])
%%ylabel(Cdc25A concentration [$\mu$M])
%%hold on, hold off
Published with MATLAB 7.11
```

A.2 Effect of P27^{Kip1} on the Dynamics of CycE/Cdk2 complex

```
 The MatLab code that simulates the effect of continous stimulation of P27$^{Kip1}$
 on the CycE/Cdk2 complex.
Codes that clear up the previous definition.
clear all % clear previously defined variable
close all % close previously opened figure window
Input codes
%%zmax=input(zmax);
%%beta=input(beta);
%%k2=input(k2);
%%b=input(b);
%%k3=input(k3);
%%gamma=input(gamma);
%%c=input(c);
```

```
%%k4=input(k4);
Codes that solves numerically.
%%disp('Solving using ode45...')
%%tic;
%%[zz,yy]=ode45(@(z,y)CyEp27,[zmin,zmax],initial condition);
Codes for plotting.
%%disp('plotting solution...')
%%clf
%%plot(zz,yy(:,1))
%%title(title)
%%xlabel('P27$^{Kip1}$ concentration [$\mu$M]')
%%ylabel('CycE/Cdk2 concentration [$\mu$M]')
%%axis([zmin zmax 0 20])
%%hold on and hold off
%%disp('Finished')
Published with MATLAB 7.11
```

A.3 Dynamics of CycE/Cdk2 complex and P27^{Kip1} Concentrations

```
 MatLab code that illustrates the dynamics of CycE/Cdk2 complex and P27$^{Kip1}$.
Clear up previous definitions.
clear all;
close all;
Input codes.
%%tmax=input(tmax); beta=input(beta);
%%k2=input(k2); b=input(b);
%%k3=input(k3); gamma=input(gamma);
```

```
%%c=input(c); k4=input(k4);
Codes for solving numerically and plotting.
%%disp('Solving using ode45...')
%tic;
%%[TT,YY]=ode45(@(t,y)CyEP27n,[tmin,tmax],[initial conditions]);
%%disp('plotting solution...')
%clf
%%plot(TT,YY(:,1),TT,YY(:,2))
%%hold on
%%hold off
%%title_str=['CycE/Cdk2 and P27$^{Kip1}$ concentrations,',
%%' $\beta$=',num2str(beta),', $\gamma$=',num2str(gamma)];
%%title(title_str);
%%xlabel('Time [min]');
%%ylabel('Concentration [$\mu$M]')
%%axis([0 tmax  0 20])
%%legend('CycE/Cdk2','P27$^{Kip1}$')
%disp('Finished')
Published with MATLAB 7.11
```

A.4 The Dynamics of the Model

```
 The MatLab code that illustrates the dynamics of the model (3.3)-(3.5).
Clear up commands.
clear all;
close all;
Input codes.
%%tmax=input(input simulation time);
%%alpha=input(alpha);
```

```
%%k1=input(k1);
%%a=input(a);
%%beta=input(beta);
%%k2=input(k2);
%%b=input(b);
%%k3=input(k3);
%%gamma=input(gamma);
%%c=input(c);
%%k4=input(k4);
Codes for solving numerically and plotting the solution.
%%disp('Solving using ode45...')
%%tic;
%%[TT,YY]=ode45(@(t,y)mod1,[tmin,tmax],[initial conditions]);
%disp('plotting solution...')
%clf
%%plot(TT,YY(:,1),TT,YY(:,2),TT,YY(:,3))
%%hold on and hold off
Codes for string and numeric changing.
%%title_str=['Cdc25A, CycE/Cdk2 and P27$^{Kip1}$ concentrations,',
%%' $\alpha$=',num2str(alpha),', $\beta$=',num2str(beta),',
%%$\gamma$=',num2str(gamma)];
%%title(title_str)
%%xlabel; ylabel;
%%axis([0 tmax  0 50]);
%%legend('Cdc25A','CycE/Cdk2','P27$^{Kip1}$')
%%disp('Finished')
Published with MATLAB 7.11
```

Bibliography

[1] Aguda B.D, *A Quantitative Analysis of the Kinetics of the G_2 DNA Damage Checkpoint System*, Proceedings of the National Academy of Sciences **96** (1999) 11352–11357

[2] Aguda B.D, *Analysis of Cancer Gene Networks in Cell Proliferation and Death*, (Information and Communication Technologies for Health, New York, 2008)

[3] Aguda B.D., and Tang T., *The Kinetic Origins of the Restriction Point in the Mammalian Cell Cycle*, Cell Proliferation **32** (1999) 321–335

[4] Aguda B.D., Kim Y., Piper M.G., Friedman A., and Marsh C.B., *MicroRNA Regulation of a Cancer Network: Consequences of the Feedback Loops Involving miR-17-92, E2F, and Myc*, Proceedings of the National Academy of Sciences **105** (2008) 19678–19683

[5] Barberis M., Klipp E., Vanoli M., and Alberghina L., *Cell Size at S Phase Initiation: An Emergent Property of the G_1/S Network*, Public Library of Science Computational Biology **3** (2007) 0649–0666

[6] Cancer Cell Reseach Group, *http://www.usyd.edu.au/wmi/cellcycle/images/imgcellcycle.jpg*, (2006) retrieved on 20th April, 2011

[7] Cangi M.G., Cukor B., Soung P., Signoretti S., Moreira G., Ranashinge M., Cady B., Pagano M., and Loda M., *Role of the Cdc25A Phosphatase in Human Breast Cancer*, Journal of Critical Investigation **106** (2000) 753–761

[8] Ciliberto A., Petrus M.J., Tyson J.J., and Sible J.C., *A Kinetic Model of the Cyclin E/Cdk2 Development Timer in Xenopus Laevis Embryos*, Biophysical Chemistry **104** (2003) 573–589

[9] Conradie R., Bruggeman F.J., Ciliberto A., Csikasz-Nagy A., Novak B., Westerhoff H.V., and Snoep J.L., *Restriction Point Control of the Mammalian Cell Cycle via the Cyclin E/Cdk2:P27 Complex*, Federation of European Biochemical Societies Journal **277** (2002) 357–367

[10] Cristini V., and Lowengrub J., *Multiscale Modeling of Cancer: An Integrated Experimental and Mathematical Modeling Approach*, (Cambridge, New York, 2010)

[11] Galaktionov K., Chen X., Beach D., *Cdc25 Cell Cycle Phosphatase as a Target of C-Myc*, Nature **382** (1996) 511–517

[12] Gantmacher F.R., *The Theory of Matrices Volume II*, (Chelsea, New York, 1964)

[13] Gardner T.S., Dolnik M., and Collins J.J., *A Theory for Controlling Cell Cycle Dynamics using a Reversibly Binding Inhibitor*, Proceedings of the National Academy of Sciences **95** (1998) 14190–14195

[14] Goldbeter A., *A Minimal Cascade Model for the Mitotic Oscillators Involving Cyclin and Cdc2 Kinases*, Proceedings of the National Academy of Sciences **88** (1991) 9107–9111

[15] Hatzimanikatis V., Lee K.H., and Bailey J.E., *A Mathematical Description of Regulation of the G_1-S Transition of the Mammalian Cell Cycle*, Biotechnology and Bioengineering **65** (1999) 060631–060637

[16] Hengst L., and Reed S.I., *Translational Control of $P27^{Kip1}$ Accumulation during the Cell Cycle*, Science **271** (1996) 1861–1864

[17] Hoffmann I., Draetta1 G., and Karsenti E., *Activation of the Phosphatase Activity of Human Cdc25A by a Cdk2-Cyclin E Dependent Phosphorylation at the G_1/S Transition*, European Molecular Biology Organization Journal **13** (1994) 4302–4310

[18] Jun-ya K., *Induction of S Phase by G_1 Regulatory Factors*, Frontiers in Bioscience **4** (1999) 787–792

[19] Keshet L.E., *Mathematical Models in Biology*, (Society for Industrial and Applied Mathematics, New York, 2005)

[20] King A.C., Billingham J., and Otto S.R., *Differential Equations: Linear, Nonlinear, Ordinary, Partial*, (Cambridge University Press, Cambridge, 2003)

[21] Kristjansdottir K., and Rudolph J., *Cdc25 Phosphatases and Cancer*, Chemistry and Biology **11** (2004) 1043–1051

[22] Mailand N., Podtelejnikov A.V., Groth A., Mann M., Bartek J., and Lukas J., *Regulation of G_2/M Events by Cdc25A through Phosphorylation-Dependent Modulation of its Stability*, European Molecular Biology Organization Journal **21** (2002) 5911–5920

[23] MathWorks, *MatLab and Simulink*, Version 7.11 (MathWorks, Massachusetts, 2010)

[24] Michaelis L., and Menten M.L., *Die Kinetik der Invertinwirkung*, Biochemistry **50** (1913) 333–369 as translated in Johnson K.A., and Goody R.S., *The Original Michaelis Constant: Translation of the 1913 Michaelis–Menten Paper*, Biochemistry **50** (2011) 8264–8269

[25] Murray J.D., *Mathematical Biology I. An Introduction*, Interdisciplinary Applied Mathematics **17** (Springer, Berlin, 2002)

[26] Norel R., and Agur Z., *A Model for the Adjustment of the Mitotic Clock by Cyclin and MPF Levels*, Science **251** (1991) 1076–1078

[27] Novak B., and Tyson J.J., *Modeling the Control of DNA Replication in Fission Yeast*, Proceedings of the National Academy of Sciences **94** (1997) 9147–9152

[28] Ohtani K., Degregori J., and Nevins J., *Regulation of the Cyclin E Gene by Transcription Factor E2F1*, Proceedings of the National Academy of Sciences **92** (1995) 12146–12150

[29] Pardee A.B, *Restriction Point Control in Human Cancer*, Tumordiagn **19** (1998) 93–100

[30] Pardee A.B., G_1 *Events and Regulation of Cell Proliferation*, Science **246** (1989) 603–608

[31] Pardee A.B., *A Restriction Point for Control of Normal Animal Cell Proliferation*, Proceedings of the National Academy of Sciences **71** (1974) 1286–1290

[32] Reed S.I., *Cyclin E: in Mid-Cycle*, BBA Biochimica et Biophysica Acta **1287** (1996) 151–153

[33] Sangdun C., *System Biology for Signaling Networks: Volume I*, (Springer, New York, 2010)

[34] Sexl V., Diehl J.A., Sherr C.J., Ashmun R., Beach D., and Roussel M.F., *A Rate Limiting Function of Cdc25A for S Phase Entry Inversely Correlates with Tyrosine Dephosphorylation of Cdk2*, Oncogene **18** (1999) 573–582

[35] Sheaff R.J., *Regulation of Mammalian Cyclin-Dependent Kinase 2*, Methods in Enzymology **283** (1997) 173–193

[36] Sheaff R.J., Groudine M., Gordon M., Roberts J.M., and Clurman B.E., *Cyclin E-CDK2 is a Regulator of* $P27^{Kip1}$, Genes and Development **11** (1997) 1464–1478

[37] Strogatz S.H., *Nonlinear Dynamics and Chaos with Applications to Physics, Biology, Chemistry and Engineering*, (Perseus Books Publishing, Massachusetts, 1994)

[38] Thron C.D., *Bistable Biochemical Switching and the Control of the Events of the Cell Cycle*, Oncogene **15** (1997) 317–325

[39] Tsihlias J., Kapusta L., and Slingerland J., *The Prognostic Significance of Altered Cyclin-Dependent Kinase Inhibitors in Human Cancer*, Annual Review of Medicine **50** (1999) 401–423

[40] Warren W., *More about Nondimensionalisation*, Lecture Notes in Mathematics (Colgate University, New York, 2005)

[41] Zetterberg A., and Larsson O., *Kinetic Analysis of Regulatory Events in* G_1 *Leading to Proliferation or Quiescence of Swiss 3T3 Cells*, Proceedings of the National Academy of Sciences **82** (1985) 5365–5369

[42] Zhilin Q., Weiss J.N., and Maclellan W.R., *Regulation of the Mammalian Cell Cycle: A Model of the G_1-to-S Transition*, American Journal of Physiology–Cell Physiology **284** (2002) C349–C364